

A THESIS REPORT ON

STUDY THE MICROSTRUCTURE AND CORROSION
BEHAVIOUR OF AGE HARDENED AA6063 ALLOY

**In partial fulfilment for the requirements of Master of Technology in
MATERIAL ENGINEERING**

Submitted by:

PRASANTA CHAKRABORTY
COURSE: M. Tech in MATERIAL ENGINEERING
Class Roll No. 002211303017
Examination Roll Number: M4MAT24012
Registration No. 163739 of 2022-2023

Under the guidance of:

Asst. Prof. Shilabati Hembram
Department of Metallurgical and Material Engineering
Jadavpur University

DEPARTMENT OF METALLURGICAL AND MATERIAL ENGINEERING
FACULTY OF ENGINEERING AND TECHNOLOGY
JADAVPUR UNIVERSITY
KOLKATA – 700032, WEST BENGAL, INDIA
2024

CERTIFICATE

This is to certify that **Mr. Prasanta Chakraborty** (Class Roll No: **002211303017** and Registration No: **163739 of 2022-2023**) is a student of M.Tech in Material Engineering at Jadavpur University, Kolkata– 700032, has been entitled a thesis work and directed to submit the final report for the partial fulfilment of the requirements for award degree of M.Tech in Material Engineering Examination at the Department of Metallurgical and Material Engineering of Jadavpur University.

During the period of final year, he has been carried out the thesis work on **“Study the Microstructure and Corrosion Behaviour of Age Hardened AA6063 Alloy”** under the guidance and supervision of Assistant Professor Shilabati Hembram and the content of this thesis report have not been submitted earlier by any other Institute by any one for award of any degree or diploma.

.....
Supervisor,
Shilabati Hembram
Assistant Professor
Department of Metallurgical and Material Engineering
Jadavpur University, Kolkata- 700032

.....
Head of the Department
Dr. Sathi Banerjee
Department of Metallurgical and Material Engineering
Jadavpur University, Kolkata-700032

.....
DEAN
Prof. Dipak Laha
Faculty of Engineering and Technology (FET)
Jadavpur University, Kolkata-700032.

DECLARATION OF ORIGINALITY AND COMPLIANCE
WITH ACADEMIC ETHICS

I hereby declare that this thesis “**STUDY THE MICROSTRUCTURE AND CORROSION BEHAVIOUR OF AGE HARDENED AA6063 ALLOY**” contains a literature survey and original research work by the undersigned candidate as a part of my M.Tech degree in Material Engineering during the academic session 2022-2024. All information in this document has been obtained and presented in accordance with academic rules and ethical conduct. I also declare that, as required by these rules and conduct, I have fully cited and referred to all material and results that are not original to this work.

Name: Prasanta Chakraborty

Class Roll Number: 002211303017

Examination Roll Number: M4MAT24012

Registration No: 163739 of 2022-2023

Place: Kolkata

Date: _____ Signature of Candidate

CERTIFICATE OF APPROVAL

The foregoing thesis, entitled as “**Study the Microstructure and Corrosion Behaviour of Age Hardened AA6063 Alloy**” is hereby approved by the committee of final examination for evaluation of the thesis as a creditable study of an engineering subject and presented by Mr. Prasanta Chakraborty (Registration No: 163739 of 2022-2023) in a manner satisfactory to warrant its acceptance as a prerequisite to the degree M.Tech in Material Engineering for which it has been submitted. It is understood that by this approval, the undersigned do not necessarily endorse or approve any statement made, opinion expressed, or conclusion drawn therein, but only the thesis for which it is submitted.

Committee of final examination for the evaluation of the thesis -

Signature of Examiners

ACKNOWLEDGEMENT

I express myself deepest sense of gratitude and obligation to my Hon'ble thesis guide **Asst. Prof. Shilabati Hembram** for her outstanding support and inspiration to initiate the thesis work and also scrutinized the report in every stage and stimulating suggestions as well as maintain my progress in track & also guiding me in achieving the objective of the thesis. It was a great experience and privilege for me to work under her in a cordial environment.

I would like to express my profound gratitude to Hon'ble **Dr. Sathi Banerjee**, Head of the Department, Department of Metallurgical and Material Engineering of Jadavpur University for permitting me to undergo this thesis work.

I am also grateful and acknowledge with much appreciation for the crucial role of the Hon'ble professors & entire team of the Metallurgical and Material Engineering Department, Jadavpur University, who made their time and resources available for my work and providing me the opportunity for undertaking the laboratory works/testing facility.

I am thankful to all friends, family members and aged mother, whose suggestions, encouragement and precious time helping me to coordinate/accomplish this work. A special thanks to all who gave me the possibility to complete this report.

This thesis work is dedicated to my father Late Mahadeb Chakraborty.

CONTENTS

S/No.	Description	Page No.
Chapter 1		
1.0	Introduction	2 - 3
Chapter 2		
2.0	Definition of Problem	5
2.1	Objectives	5
2.2	Plan of work	5 - 6
Chapter 3		
3.0	Literature Review	8 - 27
Chapter 4		
4.0	Experimental Procedure	29 -36
	Sample Selection and Cutting of Sample	
	Artificial Age-hardening	
	Sample Preparation	
	Microstructure Observation	
	Microhardness	
	FESEM, EDX, XRD	
	Corrosion Test	
Chapter 5		
5.0	Result and Discussion	39 - 61
	Chemical Composition	
	Microstructure observed by Optical Microscope	
	Microhardness Data	
	FESEM Micrographs	
	EDS Result	
	XRD	
	Corrosion Test	
	Microstructure study after Corrosion test	
Chapter 6		
6.0	Conclusion and Future Scope of Work	63
	References	64 - 66

LIST OF FIGURES

Figure No.	Description	Page No.
1	Base Sample	29
2	Sample Cutting	29
3	Size of Cut off Sample Drawing	29
4	Electric Furnace	30
5	Age Hardening Process Graph	30
6	Cloth Polishing Machine (LECO)	32
7	Optical Microscope	33
8	Microhardness Testing Machine	34
9	Sample Cutting	34
10	Scanning Electron Microscope	35
11	XRD Machine	35
12	Circuit Diagram of Corrosion Test	37
13	Corrosion Test of Autolab Instruments	37
14 - 18	Microstructures using Optical Microscope	39 - 41
19	Graphical Representation of Average Microhardness value	44
20 - 24	FESEM Images	46 - 48
25 - 29	EDS Spectrum	49 - 50
30 - 35	Crystallographic Phases using XRD	51 - 53
36	Tafel Plot of 3.5wt% NaCl Solution	55
37	Tafel Plot of 0.1M H ₂ SO ₄ Solution	56
38	Microstructure after Corrosion Test in 3.5wt% NaCl Solution	57
39	Microstructure after Corrosion Test in 0.1M H ₂ SO ₄ Solution	58

LIST OF TABLES

Table No.	Description	Page No.
1	Classification of wrought Al-Alloys	11
2	Mechanical Properties of Selected Al-Alloys 6063	12
3	Heat Treatment Designations for Al and Al alloys	13
4	Chemical Compostions of Base Materials	39
5	Microhardness Data in HV scale of Base Sample	43
6	Microhardness Data in HV scale of Sample 120°C,2hrs	43
7	Microhardness Data in HV scale of Sample 170°C,2hrs	43
8	Microhardness Data in HV scale of Sample 220°C,2hrs	44
9	Microhardness Data in HV scale of Sample 250°C,2hrs	44
10	Crystallographic Phase Analysis by XRD	54
11	Corrosion Parameters in 3.5wt% NaCl solution	59
12	Corrosion Parameters in 0.1M H ₂ SO ₄ Solution	59

Abstract

The aim of the work was to determine the effect of Age Hardening with different temperature (120°C to 250°C) of Al Alloy AA6063 (Al-Mg-Si) specimens. The experimental study is focused on Microstructural changes, Hardness and Corrosion behaviour of AA6063-T6 sample after ageing at temperature 120°C, 170°C, 220°C and 250°C with holding time two hours subsequently furnace cool.

The characterization of the sample specimens were carried out by using Spectroscopic Analysis, Optical Microscope, Scanning Electron Microscope equipped with Energy Dispersive Spectrometer (SEM/EDX), X-Ray Diffraction, Vickers Micro-hardness, Corrosion Potential Test.

The result shows Al-Mg-Si alloys (AA6063) undergo significant micro structural changes during the process before and after age hardening, also identified Under-Aged, Peak-Aged and Over-Aged temperature states with respect to observed Hardness values.

The influence of corrosion potential on heat treated AA6063 immersed in 3.5wt% NaCl solution (sea water) and N/10 molar H₂SO₄ acid solution was studied and result obtained corrosion rate higher in case of ageing sample.

Keywords: **Age-hardening, Al Alloy AA6063, Microstructure, Vickers Micro-Hardness, Corrosion Test, Under-Aged, Peak-Aged, Over-Aged Rate of Corrosion.**

CHAPTER - 1

• INTRODUCTION

1.0 Introduction:

Al-Alloy was not fully developed at the initial days of research. The process of strengthening of Al-Alloy was started by scientist Alfred Wilm in his laboratory in 1901. He was trying to discover new generation Al alloy and wanted to have strong Al-Alloys. He had background of steel, steel hardens by Quenching where Austenite phase change into Martensite phase, where missed the TTT curve. So he thought why not quenching of Al-Alloy to increase its strength. He tried quenching with alloy content Al (3.5 to 5.5) wt% of Cu. He attempted this heat treatment like steel (Heated upto certain temperature - Holding it at certain time - then Quenched with suitable cooling medium) then measure the hardness. However initially he had not succeeded and even sometimes observed decrease in hardness value. He varies the controlling parameters like temperature, holding time, quenching rate and variation of alloy content and run set of experiments several time but none of these run gave him success i.e there is no increase in hardness, he became sad.

One on a Saturday he decided to run one set of experiment again, before measuring the hardness he went outdoor for sailing. He came back on Monday and resumed his experiment, he wondered and found increasing in hardness value. Again he did control experiment deliberately waiting before measuring the Hardness value and found Hardness increasing as a function of time. Afterwards he discovered **Age hardening** concept of Al-Alloy and got patent of the Al-Alloy and process in 1906. Surprisingly he saw no change in Microstructure accompanying the increasing hardness value.

Later on gradually more research was going on to find out the real reason for increasing hardness value. It was established that Fine distribution of precipitate of intermetallic compound during **precipitation transformation process** provide more obstacle to dislocation motion resulting higher hardness value, is called **Peak Aged state**. Now it is required to explain how hardness changes as function of time and temperature. During **Overage** condition also called **Ostwald ripening**, finer distribution of precipitation transform into coarser distribution resulting reduction in hardness value. Smaller interfacial energy between precipitate into Al matrix act as a driving force during microstructure evolution from Peak-aged to Over-aged. This can be explained difference between quenching and gradual/slow cooling, in both the case stable supersaturated ‘ α ’ phase transformed into saturated ‘ α ’ phase and precipitation ‘ θ ’ phase, in case of quenching faster nucleation, slow growth resulting fine distribution of precipitation and in case of slow/gradual cooling slower nucleation, faster growth & resulting distribution will be less/coarser precipitation are form. Aging temperature should be below the solvus temperature of alloy and within the temperature range it is found that at lower temperature with longer time evaluate finer precipitation and

achieve to higher hardness value and in case of higher temperature peak hardness will achieve in shorter time with coarser precipitation and less hardness value than lower temperature. Therefore optimization of the two parameters are required to get desired result. [1]

One of the important aspect for Engineer/Designer is that significance of choosing and utilizing engineering materials for component part design and manufacturing. The majority of engineering applications satisfy service criteria, thus, before using them, their properties must be improved. Al and AA(6063) are not an exception in this scenario. [3]

In previous research works, it has been observed that aging treatment of Al-Alloy 6063 by varying aging temperature and time, material properties can be improved as compared to base material. It was established by using different characterizations technique in metallurgy harder structure can be achieved by precipitation hardening, improvement in various corrosion and wear related parameters. It was also provide general guidelines for the design and development newer materials as well as proper selection and application of existing materials.

This study was focused on understanding microstructure and corrosion behaviour and its correlation with the Hardness value when AA6063 T6 alloy artificially aged with four set of temperature ranging from 120°C to 250°C, holding time in every case is 2 hours and subsequently cooled inside furnace. The Characterizations of the base sample and age-hardened specimens have been carried out by using spectroscopy, SEM, EDS, XRD, Vickers micro hardness machine (HV), Finally, an attempt was made to correlate corrosion behaviour changes in different solutions (salt & acidic) for Al-Mg-Si alloy (AA6063) specimens subjected to different ageing condition.

CHAPTER - 2

- **DEFINITION OF PROBLEM**
- **OBJECTIVE**
- **PLAN OF WORK**

2.0 Definition of Problem:

Mechanical and Casting properties of Al are not as steel which restrict use in the transportation sector and other structural applications. These properties can be improved by adding alloying elements it with silicon and magnesium. The Al alloy 6063 is the name given to this alloy. These alloying elements improve alloy strength wear and corrosion resistance and casting ability. Due to excellent aging response, high specific strength and good corrosion resistant age-hardenable Al alloys are most preferred in the field of application. The progress of artificial hardening depends on the amount of trace elements by forming an intermetallic compound (Mg_2Si) which can precipitate as per kinetics of the alloy. In addition to that AA 6063 alloy undergo microstructural alterations during the process which profound effects on the properties of alloy. The Al-Mg-Si alloy is commonly referred to as an architectural and ornamental alloy due to its strength, simple extrudability, and high finishing quality. [2]

2.1 Objectives of the Study:

The main objective of this study aims to correlate the microstructure evolution, corrosion behaviour and hardness, considering AA6063 Al-Mg-Si alloy content as the model material which undergone artificial ageing with temperature range $120^{\circ}C$ to $250^{\circ}C$, holding time 2 hours in each case.

2.2 Plan of Work:

- i) **Sample selection:** Base Sample which has been provided heat treated (T6) Al-Mg-Si based alloy of AA6063 grade ASM standards available strip width 25mm and thickness 5 mm was supplied by private vendor.
- ii) **Sample preparation:** Sample preparation is undertaken in laboratory equipped with Sawing, automatic polishing machine through belt/cloth, Grinding, & different grade of emery paper are used for preparation of sample with required dimension and surface finish.
- iii) **Precipitation/Age-Hardening Treatment:** Considering the chemical composition of the major alloying elements (Mg and Si) of the selected material AA 6063, ageing temperatures (T_A) of $120^{\circ}C$, $170^{\circ}C$, $220^{\circ}C$ and $250^{\circ}C$ were chosen for an ageing duration of 2 hours (t_A) in each case. It was performed by using an Electric furnace in Heat Treatment Laboratory.

- iv) **Optical Emission Spectroscopy of base sample:** Compositional Analysis is carried out through optical Emission Spectroscopy.
- v) **Microstructure Study** for the given base sample and the four annealed samples and the corrosion effects on the surface by using **Optical Microscope**.
- vi) **Measurement of Micro hardness in Vickers Scale ASTM E92 of Base material & Age-hardened Sample :** by using Vickers Hardness Machine (HV scale), micro Vickers hardness measurements with a load of 200 gf and an indentation holding time of 15 sec were taken at 10 points at different locations. The average hardness values were taken.
- vii) **Scanning Electron Microscope (SEM):** A scanning electron microscope was used to study the metallographic phases of the base material four Age hardened samples.
- viii) **Field Emission Scanning Electron Microscopy coupled with Energy Dispersive X-Ray Spectroscopy (EDS/EDX):** Energy dispersive spectroscopy enables the chemical characterization/elemental analysis of materials for the given base sample and four Age hardened samples.
- ix) **Crystallographic Phase analysis by X-ray Diffraction (XRD):** X-Ray Diffractometer was used to identify materials based on their diffraction pattern and crystallographic phases.
- x) **Corrosion Potential Test:** to study Corrosion behaviour of the base material and Age hardened samples, in different solutions (salt & acidic), is expressed as the Corrosion Penetration Rate (CPR) in mm per year, or the thickness loss of material per unit of time.

CHAPTER - 3

- **LITERATURE REVIEW**

3.0 Literature Review:

3.1 General Characteristics:

Al (Al) is one of the most plentifully available metals on earth which is silvery-whitish in appearance. Al owes its excellent corrosion resistance and barrier oxide film that is bonded strongly to its surface and is highly effective in protecting the Al from corrosion. Al is passive (is protected by its oxide film) in the pH range of approximately 4 to 8.5. There are several properties that make Al one of the most widely used elements, these include; nontoxic, impervious, non-sparking, decorative, easily formed, machined, low density, corrosion resistant, electricity conductor, non-magnetic, non-combustible highly reflective heat barrier and conductor, malleable and can be easily worked. There are numerous other Al properties which are of particular use in a number of chemical and industrial applications. Al 6063 Alloy magnesium silicon based has medium strength property, and is readily suited to welding, high specific strength and stiffness, improved high temperature property controlled thermal expansion resistance, and improved wear and corrosion resistance [4].

The unique combinations of properties provided by Al and its alloys make Al one of the most versatile, economical, and attractive metallic materials for a broad range of uses—from soft, highly ductile wrapping foil to the most demanding engineering applications. Al alloys are second only to steels in use as structural metals.

Al has a density of only 2.7 g/cm³, approximately one-third as much as steel (7.83 g/cm³). One cubic foot of steel weighs about 490 lb; a cubic foot of Al, only about 170 lb. Such light weight, coupled with the high strength of some Al alloys (exceeding that of structural steel), permits design and construction of strong, lightweight structures that are particularly advantageous for anything that moves—space vehicles and aircraft as well as all types of land- and water-borne vehicles.

Al resists the kind of progressive oxidization that causes steel to rust away. The exposed surface of Al combines with oxygen to form an inert Al oxide film only a few ten-millionths of an inch thick, which blocks further oxidation. And, unlike iron rust, the Al oxide film does not flake off to expose a fresh surface to further oxidation. If the protective layer of Al is scratched, it will instantly reseal itself.

The thin oxide layer itself clings tightly to the metal and is colorless and transparent— invisible to the naked eye. The discoloration and flaking of iron and steel rust do not occur on Al.

Appropriately alloyed and treated, Al can resist corrosion by water, salt, and other environmental factors, and by a wide range of other chemical and physical agents. The

corrosion characteristics of Al alloys are examined in the section “Effects of Alloying on Corrosion Behavior” in this article.

Al surfaces can be highly reflective. Radiant energy, visible light, radiant heat, and electromagnetic waves are efficiently reflected, while anodized and dark anodized surfaces can be reflective or absorbent. The reflectance of polished Al, over a broad range of wave lengths, leads to its selection for a variety of decorative and functional uses.

Al typically displays excellent electrical and thermal conductivity, but specific alloys have been developed with high degrees of electrical resistivity. These alloys are useful, for example, in high-torque electric motors. Al is often selected for its electrical conductivity, which is nearly twice that of copper on an equivalent weight basis. The requirements of high conductivity and mechanical strength can be met by use of long-line, high-voltage, Al steel-cored reinforced transmission cable. The thermal conductivity of Al alloys, about 50 to 60% that of copper, is advantageous in heat exchangers, evaporators, electrically heated appliances and utensils, and automotive cylinder heads and radiators.

Al is nonferromagnetic, a property of importance in the electrical and electronics industries. It is nonpyrophoric, which is important in applications involving inflammable or explosive-materials handling or exposure. Al is also non-toxic and is routinely used in containers for food and beverages. It has an attractive appearance in its natural finish, which can be soft and lustrous or bright and shiny. It can be virtually any color or texture.

The ease with which Al may be fabricated into any form is one of its most important assets. Often it can compete successfully with cheaper materials having a lower degree of workability. The metal can be cast by any method known to foundrymen. It can be rolled to any desired thickness down to foil thinner than paper. Al sheet can be stamped, drawn, spun, or roll formed. The metal also may be hammered or forged. Al wire, drawn from rolled rod, may be stranded into cable of any desired size and type. There is almost no limit to the different profiles (shapes) in which the metal can be extruded [5].

3.1.1 Alloy Categories:

It is convenient to divide Al alloys into two major categories: wrought compositions and cast compositions. A further differentiation for each category is based on the primary mechanism of property development. Many alloys respond to thermal treatment based on phase solubilities. These treatments include solution heat treatment, quenching, and precipitation, or age, hardening. For either casting or wrought alloys, such alloys are described as heat treatable. A large number of other wrought compositions rely instead on work hardening through mechanical reduction, usually in combination with various annealing

procedures for property development. These alloys are referred to as work hardening. Some casting alloys are essentially not heat treatable and are used only in as-cast or in thermally modified conditions unrelated to solution or precipitation effects.

Cast and wrought alloy nomenclatures have been developed. The Al Association system is most widely recognized in the United States. Their alloy identification system employs different nomenclatures for wrought and cast alloys, but divides alloys into families for simplification. For wrought alloys a four-digit system is used to produce a list of wrought composition families as follows:

- 1xxx: Controlled unalloyed (pure) composition, used primarily in the electrical and chemical industries
- 2xxx: Alloys in which copper is the principal alloying element, although other elements, notably magnesium, may be specified. 2xxxseries alloys are widely used in aircraft where their high strength (yield strengths as high as 455 MPa, or 66 ksi) is valued.
- 3xxx: Alloys in which manganese is the principal alloying element, used as general-purpose alloys for architectural applications and various products
- 4xxx: Alloys in which silicon is the principal alloying element, used in welding rods and brazing sheet
- 5xxx: Alloys in which magnesium is the principal alloying element, used in boat hulls, gangplanks, and other products exposed to marine environments
- **6xxx: Alloys in which magnesium and silicon are the principal alloying elements, commonly used for architectural extrusions and automotive components**
 - 7xxx: Alloys in which zinc is the principal alloying element (although other elements, such as copper, magnesium, chromium, and zirconium, may be specified), used in aircraft structural components and other high-strength applications. The 7xxx series are the strongest Al alloys, with yield strengths ≥ 500 MPa (≥ 73 ksi) possible.
 - 8xxx: Alloys characterizing miscellaneous compositions. The 8xxx series alloys may contain appreciable amounts of tin, lithium, and/or iron.
 - 9xxx: Reserved for future use [5]

Wrought alloys that constitute heat-treatable (precipitation-hardenable) Al alloys include the 2xxx, 6xxx, 7xxx, and some of the 8xxx alloys. The various combinations of alloying additions and strengthening mechanisms used for wrought Al alloys are shown in **Table 1** [5].

Table 1
Classification of wrought Al alloys according to their strengthening mechanism

Alloy system	Al series
Work-hardenable alloys	
Pure Al	1xxx
Al-Mn	3xxx
Al-Si	4xxx
Al-Mg	5xxx
Al-Fe / Al-Fe-Ni	8xxx
Precipitation-hardenable alloys	
Al-Cu/ Al-Cu-Mg/ Al-Cu-Li	2xxx
Al-Mg-Si	6xxx (Heat Treated, Tensile strength 150–380 MPa)
Al-Zn/ Al-Zn-Mg/ Al-Zn-Mg-Cu	7xxx
Al-Li-Cu-Mg	8xxx

3.1.2 6xxx Series:

Alloys in the 6xxx series contain silicon and magnesium approximately in the proportions required for formation of magnesium silicide (Mg_2Si), thus making them heat treatable. Although not as strong as most 2xxx and 7xxx alloys, 6xxx series alloys have good formability, weldability, machinability, and corrosion resistance, with medium strength. Alloys in this heat-treatable group may be formed in the T4 temper (solution heat treated but not precipitation heat treated) and strengthened after forming to full T6 properties by precipitation heat treatment [9].

The 6xxx series alloys containing magnesium and silicon provide moderate strengths and good corrosion resistance in relation to other heat-treatable Al alloys. Because they are easily extruded, they are available in a wide range of structural shapes, as well as sheet and plate products. The versatility of these alloys is represented in 6061, which is one of the most commonly used Al alloys. Typically, the 6xxx alloys have good formability and good weldability. [5]

3.1.3 Cumulative Effect of Alloying Elements on Wear-Resistant:

In summary, Al wear-resistant alloys are based on alloys containing the hard, brittle silicon phase. Alloying elements such as iron, manganese, and copper increase the volume fraction of the intermetallic silicon-bearing phases, contributing to increase wear resistance compare to binary Al-silicon alloys. In addition, magnesium and copper also provide additional strengthening by producing submicroscopic precipitates within the matrix through an age-hardening process [5].

3.1.4 Mechanical Properties:

Al can be severely deformed without failure. This allows Al to be formed by rolling, extruding, drawing, machining and other mechanical processes. It can also be cast to a high tolerance. Alloying, cold working and heat-treating can all be utilised to tailor the properties of Al. The tensile strength of pure Al is around 90 MPa but this can be increased to over 690 MPa for some heat-treatable alloys. [6]

Table 2. Mechanical properties of selected Al alloys A6063 [6]

Temper	Proof Stress 0.20% (MPa)	Tensile Strength (MPa)	Shear Strength (MPa)	Elongation on A5 (%)	Elongation A50 (%)	Hardness Brinell HB	Hardness Vickers HV	Fatigue Endur. Limit (MPa)
0	100	215	140	25	24	55	55	220
0	50	100	70	27	26	25	85	110
T1	90	150	95	26	24	45	45	150
T4	90	160	110	21	21	50	50	150
T5	175	215	135	14	13	60	65	150
T6	210	245	150	14	12	75	80	150
T8	240	260	155		9	80	85	

3.1.5 Heat Treatment of Al:

A range of heat treatments can be applied to Al alloys:

- Homogenisation – the removal of segregation by heating after casting.
- Annealing – used after cold working to soften work-hardening alloys (1XXX, 3XXX and 5XXX).
- Precipitation or age hardening (alloys 2XXX, 6XXX and 7XXX).
- Solution heat treatment before ageing of precipitation hardening alloys.
- Stoving for the curing of coatings

- After heat treatment a suffix is added to the designation numbers.
- The suffix F means “as fabricated”.
- O means “annealed wrought products”.
- T means that it has been “heat treated”.
- W means the material has been solution heat treated.
- H refers to non-heat treatable alloys that are “cold worked” or “strain hardened.”
- The non-heat treatable alloys are those in the 3XXX, 4XXX and 5XXX groups. [6]

Table 3. Heat treatment designations for Al and Al alloys. [6]

Term	Description
T1	Cooled from an elevated temperature shaping process and naturally aged.
T2	Cooled from an elevated temperature shaping process cold worked and naturally aged.
T3	Solution heat-treated cold worked and naturally aged to a substantially.
T4	Solution heat-treated and naturally aged to a substantially stable condition.
T5	Cooled from an elevated temperature shaping process and then artificially aged.
T6	Solution heat-treated and then artificially aged.
T7	Solution heat-treated and overaged/stabilised.

3.2 Corrosion Potential Test:

Corrosion is gradual destruction of materials by chemical reaction with their environment, this means electrochemical oxidation of metals in reaction with an oxidant which ordinarily begins at the surface. [7]

Al is a corrosion resistant metal that naturally generates a protective coating. The coating formed is extremely thin and is generated when Al comes into contact with an oxidising environment. This protective Al oxide layer helps protect the surface of the metal from corrosion. It is fairly resistant to most acids but less resistant to alkalis. Additionally, getting surface treatment such as painting or anodising can further improve the overall corrosion resistance of the metal.

The corrosion rate, or the rate of material removal as a consequence of the chemical action, is an important corrosion parameter. This may be expressed as the **Corrosion Penetration Rate (CPR)**, or the thickness loss of material per unit of time. [7]

$$\text{CPR} = \text{KW}/\rho\text{At}$$

where W is the weight loss after exposure time t; ρ and A represent the density and exposed specimen area, respectively, and K is a constant, its magnitude depending on the system of units used.

It is convenient to classify corrosion according to the manner in which it is manifest. Metallic corrosion is sometimes classified into eight forms: uniform, galvanic, crevice, pitting, inter-granular, Selective leaching, erosion corrosion and stress corrosion.

Uniform attack is a form of electrochemical corrosion that occurs with equivalent intensity over the entire exposed surface and often leaves behind a scale of deposit. In a microscopic sense, the oxidation and reduction reactions occur randomly over the surface.

Galvanic Corrosion occurs when two metals or alloys having different compositions are electrically coupled while exposed to an electrolyte. The less noble or more reactive metal in the particular environment will experience corrosion, the more inert metal, the cathode, will be protected from corrosion.

Crevice corrosion is a form of localized attack that occurs within occluded regions or crevices of metallic components. The attack is caused by an alteration of the conditions within the crevice relative to the bulk solution. Crevice corrosion occurs when two components are joined close together to form a crevice. Corrosion occurs as the crevice accumulates water. If the crevice is small enough a differential oxygen concentration in the water can form. When this happens the base of the crevice becomes anodic to the upper region.

Pitting corrosion is a localized form of corrosion by which cavities or "holes" are produced in the material. Pitting is considered to be more dangerous than uniform corrosion damage because it is more difficult to detect, predict and design against. Corrosion products often cover the pits.

Stress corrosion cracking (SCC) is defined as the growth of cracks due to the simultaneous action of a stress (nominally static and tensile) and a reactive environment. SCC is the result of the combined and synergistic interactions of mechanical stress and corrosion/oxidation reactions. Stress-corrosion cracking occurs in a wide variety of systems. Examples include Al alloys in chloride solutions; low-alloy steels in water, caustic solutions, and nitrate solutions; stainless steels in acidic and neutral aqueous solutions; and nickel-based alloys in acidic, caustic, and neutral aqueous solutions.

Intergranular corrosion (IGC) is a form of localized corrosion characterized by preferential corrosion at grain boundaries or areas adjacent to them, with little or negligible attack on the grains. Similarly to other forms of localized corrosion, it mainly occurs on passive alloys exposed to specific corrodents. Intergranular corrosion occurs when certain metals and alloys reach temperatures between 425°C and 870°C (887°F to 1598°F.) These temperatures are most common during welding, heat treatment, or operation in high-temperature environments.

Corrosive environments include the atmosphere, aqueous solution, soils, acids, bases, inorganic solvents, molten salts, liquid metals. Testing is carried out by immersion of the

sample in solution. Corrosive immersions may be either acidic or basic and will last anywhere from 6 to 96 hours. Once the immersion cycle is complete, the sample is analysed by visual inspection or mass loss evaluation. Pitting corrosion occurs when the cathode (damaged coating) is large and the anode (exposed metal) is small. Typically the surface protection layer or film becomes the cathode when it is damaged and cracked. A small area of metal is then exposed and becomes the anodic. [7]

3.3 Applications of Al-Alloys:

Al alloys are economical in many applications. They are used in the automotive industry, aerospace industry, in construction of machines, appliances, and structures, as cooking utensils, as covers for housings for electronic equipment, as pressure vessels for cryogenic applications, and in innumerable other areas. Many applications in the mobile construction, biomedical, and textile industries have made use of anodized profiles and pieces of AA6063. [5]

Corrosion-resistant architectural Al-Alloy, also called AA6063 alloy, is primarily utilized in maritime environments. Its primary alloying constituents are silicon and magnesium, which give it good mechanical qualities overall and the ability to be heat-treated and welded. It can also be easily anodized, has a good surface finish, and is highly resistant to corrosion. [14]

3.4 Previous Research Papers related to allotted topic were studied:

3.4.1 This topic is related to Corrosion and Wear behaviour of age hardened AA6063 alloy. This study aims to correlate the abrasive wear performance with mechanical properties, considering AA6063 Al-Mg-Si alloy as the model material. The selected alloy specimens are subjected to artificial ageing at 150 °C for an ageing duration ranging from 1 to 672 h, covering severely under-aged (SUA) to peak-aged (PA) to severely over-aged (SOA) states. The lowest amount of wear rate is observed for a PA alloy with maximum hardness, while the OA alloy exhibits a slightly lower wear rate than the UA alloy at a similar level of hardness.

Aging temperature **150°C** covering severely under-aged (SUA) to peak-aged (PA) to severely over-aged (SOA) states. The hardness values to reach a maximum value of 98.00 ± 0.75 HV 2.0 after **120 h** of ageing period, this is referred to as peak-ageing (PA) state.

The solution treatment was carried out in a muffle furnace at 525 ± 2 °C for 2 h, followed by rapid quenching in an ice-water mixture. The hardness value of the alloy in the as-quenched state is measured as $\sim 43.7 \pm 1.11$ HV2.0.

The significant findings are isothermal ageing response of the selected alloy is appraised from Vickers hardness and tensile properties. The variation of mechanical properties as a function of ageing time is explained based on the evolution and transformation of precipitates with different ageing states.

Statistical analyses were performed to relate wear rate with hardness and various tensile properties considering all heat-treated alloys. It is demonstrated that wear rate decreases linearly with increasing hardness, yield strength, tensile strength, and strength coefficient; however, the same increases linearly with strain hardening exponent.

The correlations were established in this study between various wear related parameters and mechanical properties of the test material provides general guidelines for the design and development newer materials as well as proper selection and application of existing materials where abrasive performance is of prime importance [8].

3.4.2 This study is regarding the heat treatment and corrosion of Al 6063 alloy. The aim of this work was to determine the effect of heat treatment on the microstructure and the corrosion of Al 6063 alloy using weight loss method. The samples conditions were; as-cast, solution treated, supersaturated and age hardened condition. They were soaked in a 10 molar solution of sulphuric acid and monitored with time. The corrosion rate was calculated for various immersion periods. The result shows that the corrosion rate of the alloy was due to the nature of heat treatment given to the samples. Similarly, it was also found that the corrosion rate of the Al (6063) alloy was higher in the as-cast sample compared to the heat treated alloy. The passivation on the heat treated Al (6063) alloy was a little more stable therefore reducing the corrosion rate after 35 days of immersion for the aged hardened samples with **180 °C ageing time 30 min, 60 min & 120 min.**

The influence of corrosion on heat treated Al (6063) immersed in 10wt% tetra oxo-sulphate acid solution was successfully studied. The results obtained showed that the corrosion susceptibility of heat treated Al (6063) was found to be lower than the monolithic Al alloy. It was also noted that the passive films formed on the alloy was sufficiently stable which contributed in the reduction of the corrosion rate on the heat treated alloy after 35 days of immersion, therefore for applications of Al(6063) in acidic environment ageing of 30 min and 60 min was recommended. [9].

3.4.3 This topic is Wear behaviour of age-hardened 6063 Al alloy was evaluated under dry sliding conditions. A certain part of the Al samples was solution treated at 510⁰C for 2, 4, 6 and 8 h, water-quenched then aged at 180⁰C for 4 h, and the other part was solution treated at 510⁰C for 6 h, water-quenched then aged at 180⁰C for 1, 2, 3, 4 and 5 h in a muffle

furnace. The as-cast and the aged samples were fully characterised before and after the wear testing using hardness, profilometer, scanning electron microscopy (SEM), optical microscopy, X-ray diffraction, and energy dispersive detector (EDS). The wear tests using on a pin-on-disc machine showed that the aging treatments improved the wear behaviour of AA 6063 alloy compared to as-cast samples.

The artificial aging produces the harder structure. The microstructure was altered with the aging treatment, and it was observed that the precipitates in the structure dispersed finely with the increasing of the aging time [10].

3.4.4 This study was found on wear behaviors of aged Al AA 2024 and AA 6063 alloys were investigated. AA 2024 and AA 6063 Al alloys were solution treated at two different temperatures of 490°C and 520°C. Then all samples were cooled to room temperature. After this process, the samples were aged at three different temperatures (140°C, 180°C and 220°C) for five different periods of time (2, 4, 6, 8, 10) hrs. The microstructures of the aged samples were examined by optical microscope, SEM-EDS and X-ray analysis. The hardness values of the aged samples were measured by micro hardness tests. Wear tests were carried out on the pin-on-disc model wear test apparatus under sliding velocity at 2 m s⁻¹ speed, 400, 800, 1200 and 1600 m sliding distances for 10, 20 and 30 N variable loads. The mass-loss values of the aged samples were tested by wear tests. As a result of this study, the hardness of the second phase precipitated samples was found to be higher than that of the as-cast samples and it increased with increasing the solution temperature and aging periods. The study also revealed that the wear rate and friction coefficient can be decreased with increasing the solution temperatures and aging periods.

It was determined that AA 2024 alloys had higher hardness values than AA 6063 alloys. It was determined by hardness measurement that the hardness value of the heat treated aged sample of AA 2024 and AA 6063 alloys was higher than the samples which are not aged.

It was also determined that the temperature and period of aging decreased the resistance of the material and its hardness value after a certain level. It was specified that reason of this could be the decrease of hardness value of the material in the course of time as a result of the fact that precipitations formed in the structure increased to the amount that cannot prevent the dislocation movement.

The highest hardness values of AA 2024 Al alloys were obtained when the samples were aged at 180 °C. 175.8 HV hardness value was obtained in the sample which was aged for 14 h. Hardness increased with the aging process. The reason for the increase in hardness is due to the formation of CuAl₂ and AlCuMgSi precipitations. An excessive aging occurred at 220 °C, and as a result there was a decrease in hardness values.

The highest hardness values of AA 6063 Al alloys were obtained when the samples were aged at 180°C. An increase in hardness was also observed as a result of increasing the aging periods at 140°C. However, 100 HV value was reached at 180°C and in 14 h. This increase in hardness is due to the formation of Mg₂Si, AlFeSi and on a limited scale CuAl₂ precipitation. As there is an excessive aging at 220°C, the hardness values are lower.

After the excessive aging, a decrease was observed in wear resistance of AA 2024 Al alloys. The highest mass loss was obtained in samples which were aged at 220 °C. On the other hand, the highest wear resistance was obtained in AA 2024 Al alloy samples, whose hardness values are the highest and which were aged at 180 °C. There was a decrease in the mass loss with increasing the aging period. This is due to the effect of aging process.

There was a more mass loss in AA 6063 Al alloy than in AA 2024 alloy. Because the hardness values of AA 6063 alumunium alloy samples increased with increasing the aging period, the mass loss decreased. There was not too much change in the mass loss in the wear test results of the samples aged at 220°C [11].

3.4.5 This topic is related to Influence of aging parameters on the mechanical properties of 6063 Al alloy was studied. The 6063 Al alloy were given various heat treatments at under-aged, peak-aged and over-aged temperatures. The effect of precipitation on the tensile strength, yield strength, hardness, ductility and number of cycles required to fail the alloy at constant stress was investigated. The variation in time and temperature have improved the mechanical properties of the Al-alloy, whereas the ductility has decreased. The experimental work has revealed that time and temperature play a very important role in the precipitation hardening process of the Al-alloy. The initial increase in the tensile strength, yield strength, hardness and fatigue is due to vacancies assisted diffusion mechanism and formation of high volume fraction of guinier preston (GP) zones, which disturbs the regularity in the lattices. In over-aging of the alloy, the size of the individual particle increases, but the number of particles decreases. This causes few obstacles to the movement of dislocations, therefore, the mechanical properties decreases. The scanning electron microscope (SEM) study of the under-aged alloy have exhibited facet fatigue fracture surface, whereas the peak-aged and over-aged alloy show a mixed mode of fracture, i.e. facet fracture with striation and also intergranular fracture.

A complex sequence of time and temperature dependent changes is responsible in precipitation hardening of 6063 Al alloy. The experimental results have revealed that aging between 8 and 10 h at 448 K is the most suitable combination of time and temperature imparting maximum tensile strength, yield strength and hardness to the alloy. Aging at 473 K for a period of 6 h has produced maximum resistance to fatigue fracture behaviour in the alloy.

The initial increase in the above mechanical properties, is due to vacancies assisted diffusion mechanism. At room temperature and high temperatures, i.e. under-aged and peak-aged condition the vacancies are highly mobile. These vacancies play a significant role in the formation of GP zones, which are considerably rich in solute atoms. The local segregation of solute atoms produces a distortion of the lattice planes both within the zones and extending for several atomic layers in the matrix. With an increase in number/density of zones, the degree of disturbance of the getting regularity in the lattice increases. Therefore, the mechanical properties as well as the fracture behaviour of the alloy are enhanced. The strengthening effect can also be as a result of interference with the motion of dislocation, due to the formation of precipitates in under-aged and peak-aged conditions. The peak-aged alloy has the highest mechanical properties compared to the under-aged and over-aged 6063 Al alloy. A decrease in the mechanical properties of the alloy in the over-aging conditions (increase in aging time and temperature) has occurred because of coalescence of the precipitates into larger particles, bigger grain size, and also due to annealing of the defects. This will cause less obstacles to the movement of dislocations and hence the mechanical properties starts to decrease. A similar behaviour is also observed in the SEM photomicrographs i.e. the under-aged alloy exhibits facet fatigue fracture and the peak-aged and over-aged alloy show a mixed mode of fracture, i.e. facet fracture with striation inter-granular fracture. [12]

3.4.6 This paper is regarding Corrosion Behaviour of type AA6063 Al Alloy on High Pressure Gas Cylinders for Oil and Gas Application. In the oil and gas industry, one of the biggest challenges is the effluence of CO₂, air, oxygen, and special gases, as well as contamination in compressed gas cylinders during storage and transportation, which causes localized pitting corrosion of the metal handling and storing. Using the weight loss method and the potential-dynamic polarization test, the inhibitory influence of ketoconazole (KCZ) drug performance on the electrochemical corrosion behaviour of type AA-6063 aluminum alloy in 1M H₂SO₄ solutions was investigated in an effort to address this. Inhibitor concentrations between 0.1 and 1.0% g/v were taken into consideration. According to the weight loss and potentiodynamic polarization tests, the medication compound exhibited an average ketoconazole drug inhibition efficiency above 50% in H₂SO₄ acid, indicating its effectiveness in acid solutions.

Because of its low cost, light weight, excellent electrical and thermal conductivity, and strong resistance to corrosion in a wide range of hostile conditions, Al is a desirable material for engineering applications. Al resists corrosion in corrosive settings because an invisible oxide film forms a protective layer that adheres tightly to the metal's surface. The

coating lessens or stops corrosion and is stable in solutions with pH ranges of roughly 4.5–8.5 (in bases and acids). The metal exhibits a high rate of corrosion and dissolving in strong acidic or alkaline solutions because of the film's solubility in these environments.

The results obtained demonstrate that the electrochemical properties of KCZ medication outperformed highly derivative organic drug in terms of corrosion inhibition of type AA-6063 Al in 1 M H₂SO₄ acid. It was found to be of mixed kind, with a noteworthy 60% inhibitor efficiency. It is determined that the KCZ compounds' activity of the functional groups and enough molecules is what causes the inhibitory action. The Langmuir and Frumkin adsorption was preferred by the adsorption isotherm fit. [13]

3.4.7 In Marine Application, Aging Treatment to increase the Erosion-Corrosion resistance of AA6063 Alloys. AA6063 alloys are commonly employed in shipbuilding and boat construction. Erosion and corrosion can occur on a moving ship made of Al alloy submerged in saltwater. A corrosive fluid's relative velocity causes erosion-corrosion, an accelerated corrosion assault on metals. Therefore, the Al alloy's erosion and corrosion resistance need to be improved. The AA6063 alloys were cast in order to prepare them for this work. After six hours of solutionization at 535°C, the alloys were water-quenched. After five hours of artificial aging at 200°C, the alloys were left to age naturally for a period of fourteen days. Tests for erosion and corrosion were conducted using a 3.5 wt% NaCl solution. A magnetic stirrer with rotational speeds of 100, 200, 300, 400, 500, and 600 was used to agitate the mixture.

Corrosion-resistant architectural Al-Alloy, also called AA6063 alloy, is primarily utilized in maritime environments. Its primary alloying constituents are silicon and magnesium, which give it good mechanical qualities overall and the ability to be heat-treated and welded. It can also be easily anodized, has a good surface finish, and is highly resistant to corrosion; nevertheless, in a maritime environment, it is more vulnerable to corrosion attack. The Al alloy may experience pitting corrosion due to ion Cl⁻ in seawater. Corrosion and erosion of an Al alloy ship in motion are commonplace. As a result, the American Society for Testing and Material (ASTM) and the American Bureau of Shipping (ABS) have determined that shipbuilding can benefit from the use of A6063 Al alloy with solution heat treatment and artificial aging (T6).

The most common type of erosion-corrosion is seen in soft alloys, such as copper, Al, and lead alloys. In a corrosive environment, alloys that form a surface film typically have a limitation velocity above which corrosion accelerates rapidly. It is well known, a solution heat treatment can strengthen the metals' resistance to corrosion. The

mechanism of metal erosion and corrosion in marine environments suggests that the surface of a metal object might be harmed by its relative motion in water.

When age hardening begun, both magnesium and silicon began to separate from the solid solution and precipitate as Mg₂Si. Early precipitation was entirely consistent with the Al matrix. Mg₂Si precipitates will eventually become somewhat coherent and incoherent at high temperatures, the purpose of this study is to ascertain how AA6063 Al's resistance to erosion and corrosion is affected by solution heat treatment, artificial aging and natural aging. Because of the various heat treatments, the alloy's hardness will be correlated with its corrosion resistance and erosion resistance, as indicated by the corrosion rate.

The aim of this work was to determine the effects of solution heat treatment, artificial aging, and natural aging on the erosion and corrosion resistance of A6063 Al. The corrosion rate indicates how the alloy's durability against corrosion and erosion is associated with its hardness due to the different heat treatments. [14]

3.4.8 This paper is related to corrosion behaviour of Al-12Si-1Mg automotive alloy in acidic, alkaline and salt media where Zr traces. Al alloys containing silicon are very important among the majority of casting alloys. They are widely used in the automotive and aerospace industries. This is mainly due to the outstanding effect of silicon in the Al alloys referring to the improvement of the casting characteristics and the corrosion resistance as well as with other mechanical properties. It also improves the fluidity, the hot tear resistance and the feeding characteristics. Sometimes other alloying elements such as magnesium, copper, nickel, manganese, tin, etc. are added to the alloys aiming an intended application. It is necessity to study the corrosion resistance and the mechanical properties of the alloys because they are used in different environments. Because corrosion is an ongoing process, it may be challenging to stop. It is a damaging occurrence that takes place in almost every setting. It results from an electrochemical reaction between the aqueous phase and the metal or alloy.

The oxidation of metal ions and the reduction of the depolarizer in the medium hydrogen ions to hydrogen gas in an acidic medium or oxygen to hydroxide ions in neutral and alkaline media occur simultaneously and cause metal corrosion. A metal's physical characteristics and mechanical behaviour are also altered by corrosion processes, in addition to its chemical properties. In a neutral aqueous solution, Al and its alloys make excellent corrosion-resistant materials.

Because a passive layer forms, Al and its alloys are excellent corrosion-resistant materials in a neutral aqueous solution. The mechanical properties of Al alloys can be effectively enhanced by the inclusion of transition elements like Zr and Ti. It has been

discovered that Al and trace elements can combine to generate dispersoids, which govern the grain boundary structure and enhance the alloy's resistance to recrystallization. It has been stated that the precipitated phases and refined microstructure affect the Al alloys' ability to withstand corrosion.

Numerous elements pertaining to the metal and environment have an impact on corrosion. The corrosion behaviour is also significantly influenced by the type of the corrosive media. The current work uses the weight loss method to examine the inhibitive and adsorption characteristics of the Al-12Si-1Mg automotive alloy in H_2SO_4 , $NaOH$, and $NaCl$ media. The goal of the research is to examine how Zr traces affect the alloy's corrosion behaviour.

Based on a thorough examination of the data, it can be concluded that the segregation of alumina particles in the matrix and the progressive breakdown of passive films cause the Al-12Si-1Mg automotive alloy to corrode more quickly in an acidic solution than in an alkaline one. Because of the passive layer deposition on the surface, the alloys show higher corrosion resistance in a salt media. There were no appreciable variations in the corrosion behaviour of the Zr-containing alloy across all corrosive media examined. A black corrosion product layer forms in alkaline and salty environments, increasing the alloy's resistivity; in acidic media, an intense pit formation is noted. In a salted media, Al oxide creates a very thin coating. Resistivity decreases as a consequence for up to 47 days of exposure, there is no sign that crystallographic pitting has formed in the $NaCl$ solution. [15]

3.4.9 This study is effect of microstructure on corrosion behaviour of Al-Alloys. The intricate process of pitting corrosion in Al alloys can be influenced by a number of variables, including the alloys' chemical composition and microstructure. The primary elements that significantly impact the corrosion of Al alloys are the distribution of second phases within the alloy and the electrochemistry of the alloy.

The goal of this work was to further our understanding of how an Al alloy's microstructure and chemical makeup affect both its susceptibility to localized corrosion and its ability to create a passive layer. Alloy samples from 3003, 5049, 6061, and 6063 were created in order to conduct the experiment. The corrosion potential of the alloys under investigation was examined using the open circuit potential transient technique. Potentiodynamic polarization measurement was used to determine the corrosion parameters, such as corrosion potential, and the capacity of alloys to form the passive layer. This study used the salt spray test to investigate the corrosion behaviour of alloys as a function of time. It was taken into consideration 26 samples of each kind of alloy, which were made from tubes

and tested over the course of 49 days in a salt spray chamber. Two samples of each alloy were removed from the chamber at predetermined intervals. This test was used to evaluate the type and rate of corrosion. Since pitting is the primary corrosion process, optical microscopy was used to quantify the depth of the 10 deepest pits. Also, the cross section of the deepest pit was analysed to see if the alloy is susceptible to intergranular corrosion.

Statistical analysis was carried out in order to investigate the variation of corrosion rate during exposure and to predict the lifetime of a component. In particular, the Extreme Value theory, the Gumbel distribution, was employed to plot the probability paper of the extreme pit depth occurrence. In addition, the Gumbel distribution theory was utilized to extrapolate data to longer exposure times. Al and its alloys constitute a significant class of materials because of its great technological worth and numerous industrial uses, particularly in the marine industry. With the exception of pitting corrosion caused by certain reactive species, Al and its alloys are typically passive and resistant to corrosion in aqueous solutions. In the pH range of 4 to 9, the surface oxide layer on these materials remains stable. Aggressive anions, such as the chloride ion, cause more rapid lm breakdown and corrosion. Many grades of Al and diverse materials were used in a comprehensive study to examine the effect of alloying elements on the disintegration of the passive film. It is known that the presence of alloying elements in the microstructure, such as single elements (Cu, Si) or insoluble intermetallic particles, causes small electrochemical cells to form between the Al matrix and them. By pitting in an aggressive media, this results in a severe and highly localized assault. The intermetallic phases' electrochemical makeup is a major factor in how susceptible an Al alloy is to localized corrosion.

In this work, electrochemical measurements and a salt spray test were used to assess the corrosion behaviour of four different types of Al alloy. Then, the extreme value theory was used to statistically analyse the Pit depth data. These inferences can be made based on the findings. It was discovered that the chemical composition and microstructure of alloys 3003, 5049, 6061, and 6063 were related to their corrosion behaviour. OCP experiments demonstrated that alloy 3003's high Mn content causes it to corrode at a more positive potential in both NaCl and SWAAT solutions. The alloys 5049, 6061, and 6063 showed a greater negative OCP, which is related to the Mg concentration of these alloys. When comparing the OCP of alloys 5049 and 6xxx (which were the subject of this project) to alloy 3003, there is no discernible difference that can be attributed to the alloys' lower Mn and greater Mg contents. The alloy 5049 demonstrated a high level of corrosion resistance with its broad passive region and low corrosion current density. In the NaCl solution, alloy 3003 showed a very high corrosion current density and a short passive zone, indicating limited

corrosion resistance. Alloy 3003 corrodes with a relatively high rate, according to the salt spray test. Because alloy 3003 contains Cu, intergranular corrosion was also seen in addition to pitting. Alloy 5049 has the least corrosion of all the alloys under study. The second resistant alloy was alloy 6061.

Potentiodynamic polarization results agreed with corrosion test results for all the alloys studied. In synthetic saltwater solutions, the ability to build passive film on the surface is generally enhanced by magnesium content, leading to good corrosion resistance. Conversely, Cu and Fe-containing microstructure particles make alloys less resistant to corrosion.

The data acquired for the alloys 3003, 5049, and 6063 subjected to an acidic saltwater solution were well fitted by the Gumbel extreme value distribution. A helpful model for estimating how long an alloy component would last when exposed to seawater is the Gumbel distribution. With alloy 6061, the Gumbel distribution for smaller pits and another full probability distribution for extreme pit depth are bi-modal for prolonged exposure times. [16]

3.4.10 This paper is regarding corrosion behaviour of Al and AA6063 in phosphoric acid medium (H_3PO_4 , strength 0.5M, 1M, 2M). In phosphoric acid at varying concentrations and temperatures, the corrosion behaviour of Al and 6063 Al alloy was studied by electrochemical impedance spectroscopy (EIS) and Tafel polarization techniques, the study was conducted utilizing an electrochemical approach. By applying Arrhenius theory and transition state theory, the thermodynamic and kinetic parameters were computed. Analysing the surface morphology was done with an energy dispersive X-ray (EDX) and scanning electron microscopy (SEM). With an increase in acid concentration and temperature, both materials corroded more quickly. It was discovered that the corrosion rate of 6063 Al alloy was greater than that of pure Al. The corrosion of Al and the 6063 Al alloy in phosphoric acid medium was found to have a suitable mechanism. There was a strong correlation between the outcomes from the Tafel polarization and electrochemical impedance spectroscopy (EIS) methods.

In addition to causing a direct financial loss, corrosion is a major issue since it undoubtedly accelerates the depletion of our natural resources. The necessity to preserve the world's metal resources has brought increased attention to corrosion research. Because metals are being used in more and more technological applications, there is a greater focus on controlling metallic corrosion these days. Because of the significance of technology and the wide range of industrial uses for Al, researchers have focused a great deal of emphasis on the corrosion of Al and Al alloys. In terms of production and consumption, Al comes in second

to iron. Applications for Al and its alloys include automotive, aircraft, home appliances, containers, and electronics.

Al and its alloys have become popular substitute materials in the chemical processing and aerospace industries. Because Al naturally forms a passivating oxide layer, Al and its alloys are used in a wide range of applications. Nevertheless, the protective layer disintegrates in the harsh, corrosive environment, causing the material to corrode. According to reported literature, in-depth research is done on the corrosion behaviour of Al and Al alloys in solutions containing sulfuric and hydrochloric acids. One common industrial chemical used for electropolishing and acid cleaning Al is phosphoric acid. Phosphoric acid corrodes Al and its alloys even though the rate of dissolution of Al in it is less than that of hydrochloric or sulfuric acid. Additionally, phosphoric acid is utilized in the pickling of expensive, fragile parts and precision objects where it is necessary to prevent rerusting after pickling.

The literature that is currently available indicates that not much research has been done on how Al and 6063 Al alloy corrode in phosphoric acid medium. Here investigating the corrosion behaviour of Al and its alloys in various media and the application of green inhibitors to control corrosion in the same. Here, they present the findings of the corrosion behaviour of Al and the 6063 Al alloy at various temperatures and concentrations in phosphoric acid medium.

When compared to 6063 Al alloy, pure Al corrodes less in phosphoric acid medium. The rate of corrosion increases as the concentration of phosphoric acid increases. Tafel polarization and EIS study results show strong agreement with one another; the rate of corrosion in both metals rises with temperature. [17]

3.4.11 This paper tells about Surface and corrosion properties of AA6063-T5 Al alloy in Mo-containing NaCl solutions. The corrosion characteristics of Al alloy AA6063-T5 were examined in NaCl solutions containing molybdate. Experiments using electrochemistry, microscopy, and spectroscopy were used to investigate the mechanism of molybdates' suppression of corrosion. The data obtained from SEM-EDX, magnetic force, and intermodulation electrostatic force microscopy indicated a preference for the inhibition initiation over Fe-rich cathodic IMPs. Spectroscopic analysis revealed that mixed Mo (VI, V, and IV) species make up the surface layer that has formed. After 4 hours of treatment, this layer produced inhibition with an effectiveness of about 90%. Approximately 70% effectiveness was attained even following a week of exposure. It was suggested that aqueous molybdates suppress corrosion by a two-step oxidation-reduction process. One of the main causes of the shorter lifespan and early failure of metallic-based structures and components in

everyday applications and technologies is corrosion phenomena. Because they are used so often, Al alloys are prone to corrosion. Pure Al has a relatively strong corrosion resistance because of the adherent and dense oxide coating that forms spontaneously. On the other hand, the surface layer of Al alloys has a lot of heterogeneities, like intermetallic particles (IMPs). Because these IMPs produce local cathodes or anodes in the microstructure of the material, they make the material more prone to localized corrosion. Because of this, protecting Al alloys from corrosion is crucial and necessitates the creation of several protection techniques.

One popular method for stopping the corrosion of metallic items is to employ corrosion inhibitors. Chromate has proven to be an effective inhibitor for Al alloys because of its adaptability, high inhibition efficacy, and capacity for self-healing. Chromatones, however, are mutagens and carcinogens. Thus, the creation of novel, effective, and ecologically friendly inhibitor substitutes has received attention lately. Oxyanions of the transition metals from the periodic table's VB–VIIB groups have been thoroughly studied in this context. Vanadates and molybdates among them demonstrated the greatest ability to successfully lower the rate of corrosion of Al alloys. Because they are less hazardous, molybdates are more promising from an environmental standpoint. The fact that molybdates can shield pure Al, something vanadates cannot do, further demonstrates the adaptability.

In this study, we looked at how molybdate affected the Al AA6063-T5 alloy's resistance to corrosion. The alloy's microstructure and the Mo-rich layer's composition were linked to the electrochemical data. The ensuing deductions are made:

i). Multiple micrometer-sized IMPs are seen in the microstructure of AA6063-T5. The electrochemical cathodic character of IMPs was shown by IMEFM studies, which led to a high susceptibility to micro-galvanic corrosion between the IMPs and the Al matrix.

ii). Electrochemical results showed that the AA6063-T5 alloy's corrosion rate is significantly reduced when 3 mM $(\text{NH}_4)_6\text{Mo}_7\text{O}_{24}$ is added to an aqueous 0.05 M NaCl solution. Within a day of exposure, molybdate exhibits varied effects on corrosion inhibition, with an inhibition efficiency of roughly 90%.

iii). The commencement of the inhibitory process over micrometer-sized cathodic IMPs was revealed by surface analysis. The final surface film has two distinct regions: a black core with Mo(V) and Mo(VI) compounds, and a yellow perimeter with Mo(IV), Mo(V), and Mo(VI) compounds. While a significant portion of the latter contained amorphous polymerized species, the former was composed primarily of crystalline molecules.

iv). The process by which $(\text{NH}_4)_6\text{Mo}_7\text{O}_{24}$ inhibits the corrosion of AA6063-T5 in an aqueous

0.05 M NaCl solution proceeds in multiple stages. First, the adsorbed Mo (VI) species over cathodic IMPs are reduced to Mo (IV) due to Al matrix corrosion around the IMPs. This is followed by an oxidization that forms mixed-valence Mo (V) and Mo (VI) compounds. [18]

3.4.12 This study examines the impact of cooling rate on low-grade cold deformation–recrystallization properties during homogenization treatment of aluminum alloy AA 6063. For this reason, material from billets made using the semi-continuous casting method was used to create tapered tensile test specimens, with one side measuring 10 mm in width and the other 18 mm. These samples underwent six hours of homogenization at 560 °C and five different speeds of cooling. There are three specimens per group. After undergoing a tensile test to determine the deformation gradient, these specimens were annealed for one hour at 450, 500, and 550 degrees Celsius. Metallographic analysis was performed on the specimens after these treatments. Research results indicate that a rise in cooling rate led to a rise in critical strain and a fall in the maximum grain size. During homogenization treatment, metallographic measurements showed that the cooling rate directly affects the particle size, interparticle spacing, and volume fraction of the particles, decreasing them.

Certain compounds, such CuAl₂, Mg₂Si, contain alloying elements added to Al, such as Cu, Mg, and Si, during the solidification process. Certain parts of the matrix may see an accumulation of those brittle and hard chemicals. There are softer areas of the matrix and harder, more brittle areas. The mechanical properties of a material vary depending on the hardness of its distinct areas. Heat treatment for homogenization can solve this issue. If the material is to be plastically deformed, homogenization must be given to it after casting. One cannot obtain items of superior quality from an unhomogenized Al billet. Heat treatment known as homogenization creates a homogenized matrix in which balanced chemical accumulation occurs. The outcome of the study is as follows:

Modifying the homogenization treatment's cooling rate can alter the AA 6063 material's low cold deformation–recrystallization characteristics. As the cooling rate increased, the size of the Mg₂Si particles decreases and the critical deformation rate increases. The annealing temperature of the AA 6063 material reduced the maximum grain size. As the annealing temperature increased, the critical deformation rate reduced and the maximum grain size increased. [19]

CHAPTER - 4

- **EXPERIMENTAL PROCEDURE**

4.0 Experimental Procedure:

4.1 Sample Selection:

Base Sample utilized in the present study are heat treated (T6) Al-Mg-Si base alloy of AA6063 grade ASM standards available strip width 25mm and thickness 5 mm. Chemical Compositions of the Al-Alloy 6063 was obtained by spectroscopic analysis, make by BRUKER, Model Q8-MAGELLAN at Metal and Steel Factory, Ishapore.



Figure 1: Base Sample (25mm x 5mm)

4.2 Cutting of Sample:

In first step, 5mm thick samples were sectioned off from above strip with width 10 mm each to make five rectangular shape specimens by using the Struers Secotom-20 abrasive cutter for the purpose of annealing of four different temperature (120°C, 170°C, 220°C and 250°C) subsequently studying the optical microstructure.

It is important to fact that the cutting method of a specimen may change the actual microstructure of the material for example, excessive heating, chemical attack, or amount of mechanical damage should not be happened during cutting. Therefore, during cutting feeding of appropriate coolant, firmly mounting of work piece by using appropriate fixture and setting of cutting tool were taken care off to prevent such type of occurrence.



Figure 2: Sample Cutting (25mm x 10mm x 5mm)

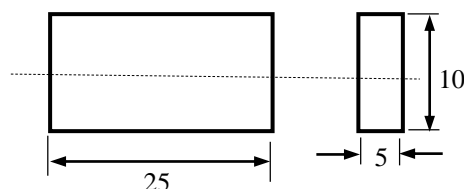


Figure 3: Size of Cut off Sample (25mm x 10mm x 5mm)

4.3 Artificial Age Hardening:

Four prepared rectangular size samples having 25 mm length, width 10mm and 5 mm thickness were subjected annealing heat treatment in an Electric Furnace (Make: THERELEK, Voltage 230V, 4 KW, Maximum Temperature 1000°C) at Heat Treatment Laboratory . One specimen was heated inside the furnace from room temperature to **120°C** at a slow heating rate and were held at that temperature for **2 hours** (120 min) with a 10 min stabilization time. The temperature displayed by the furnace was monitored by a K type (Chromel-Alumel) thermocouple to which cold junction correction was applied to account for the effect of ambient temperature. After the soaking period was over the sample allow cool inside the furnace upto an ambient temperature of 28°C. Afterwards, it was removed from the furnace. Similar process was repeated for other three samples with temperature **170°C, 220°C and 250°C with soaking period 2 hours (120 min)**.



Figure 4: Electric Furnace

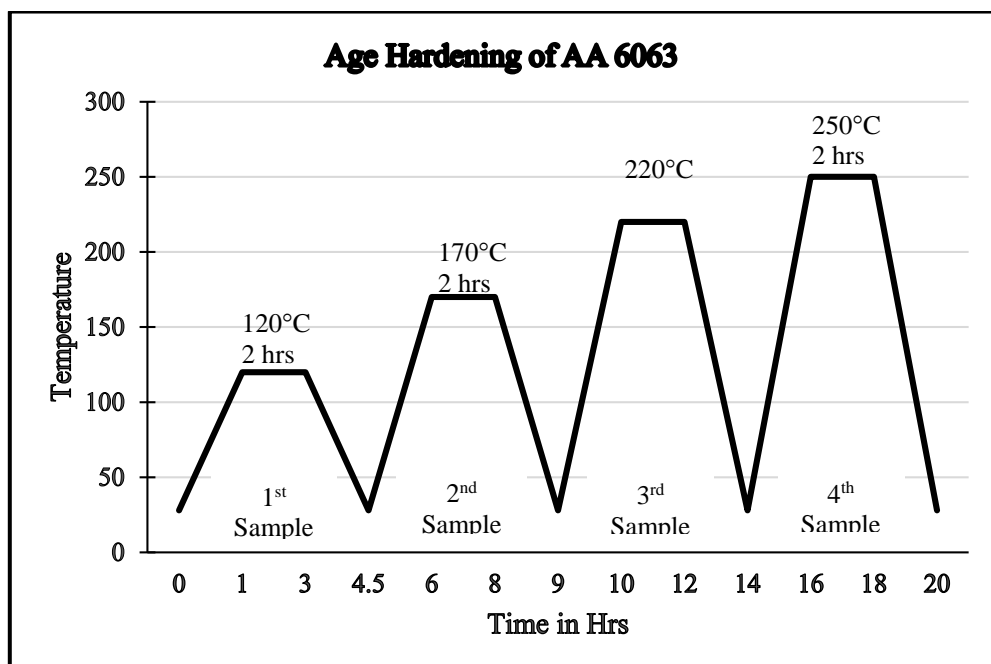


Figure 5: Age-Hardening Process

4.4 Sample Preparation:

Samples preparation for optical microscopy were carried out through different stages. It was important to ensure that surface preparation of the specimen should be mirror polished without unevenness or scratches on the surface to obtain satisfactory microstructural image. The variation in material surface may affect microstructure of one sample, so preparation of sample for microscopy was very important aspect. It was experienced difficulties to achieve true surface of a sample where manual polishing is involved for example, very soft or ductile materials got deform to polish mechanically also. For this purpose various stages of abrasion procedure were adopted for preparation of the samples under study with different orientation and finally cloth polishing followed by etching were performed.

4.4.1 Grinding

Surface layers damaged by cutting and excessive roughness on the surface was removed by grinding. Specimens were ground with belt conveyor mounted with emery paper (60 grit number) and a suitable coolant water was applied to remove debris and heat.

4.4.2 Paper Polishing:

For the purpose of surface polishing of samples silicon carbide paper were used and performed by manually on the wooden table. The coarseness of the paper is indicated by a number, the number of grains of silicon carbide per square inch. So, lower to higher the number indicate coarser to finer emery paper for example, 1200-grit paper is finer than 400. The grinding procedure involves several stages, using finer paper (a higher number) for each successive stage. Each grinding stage removes the scratches from the previous one. This was achieved by orienting the specimen perpendicular to the previous scratches, and observing for these previously oriented scratches to be obliterated. Between each grade, the specimen was washed thoroughly with soapy water to prevent contamination from coarse grit present on the specimen surface. Typically, available coarser to finest grade of papers used progressively were 120, 180, 400, 800, 1200, 1500, 2000, 2500, and 3000. Paraffin was spread over the paper for smooth polishing and act as a lubricant to prevent heat and avoid accumulation of the debris on the rubbing surface. Finally the specimens were thoroughly rinsed with water, followed by alcohol and then allowed to dry.

4.4.3 Cloth Polishing:

Polishing discs were covered with a soft cloth impregnated with abrasive diamond particles. Particles of two different grades were used: a coarser polish diamond particles, typically with microns in diameter, which should remove the scratches produced from the finest grinding stage, and finer polish diamond particles, typically with diamond particles of 1 micron in diameter, to produce a very smooth surface. Before using a finer polishing wheel, the specimen should be washed thoroughly with warm soapy water followed by alcohol to prevent contamination of the disc as debris can become embedded in the surface. Alumina (Al_2O_3) paste (grit size $0.25 \mu\text{m}$) was applied during polishing to obtain a scratch free mirror-like finish and water being continuously fed over the specimen during polishing. Cloth polishing was carried out till scratches are removed fully from the surface of the specimen and was ensured by viewing it under optical microscope.



Figure 6: Cloth Polishing machine (LECO)

4.4.4 Etching:

Etching was carried out to reveal the prominent microstructure of the metal surface through a selective chemical attack to the preferentially high energy sites and also removes the thin deformed layer introduced during polishing. In alloys with more than one phase present, etching creates contrast between different regions through differences in topography or reflectivity.

The polished surface was etched using **Kellers etchant (in 100 ml solution, 2.5 ml HNO_3 , 1.5ml HCl , 1 ml HF , 95 ml distilled water)** which was prepared carefully and kept in a small glass container. This was applied using a cotton bud wiped over the surface a few times and the specimen immediately rinsed with distilled water and washed in alcohol

and dried with the help of a drier. Precaution was taken not to over-etched which may lead to obscure the main features trying to be observed. A small piece of paper or cloth covers always used so that the surface of the specimen free from hand contamination and also to avoid further scratching. Now the samples were ready to imaging microstructure under optical microscope.

4.5 Microstructure Observation using an Optical Microscope:

The five specimens of AA 6063 (one Base sample, four age hardened 120°C, 170°C, 220°C and 250°C sample) for the test were metallographically polished and etched before microscopic examination. A metallurgical optical microscope with accessories was used to capture optical micrograph image with different magnification. The **Machine used Model LEICA DM2700 M coupled with a digital camera interfaced with a personal computer using a software LASV 12.4.**

Ideally, the surface to be examined optically was kept flat and level by mounting the specimen into plastic clay which was placed on a microscope glass slide under the lens. The slide was levelled by adjusting levelling wheels and whole field of view were taken in focus for image clarity.



Figure 7: Optical Microscope

4.6 Microhardness Measurement:

After optical microscopy imaging, five samples (one base and four annealed) were undergone micro-hardness test by using Vickers hardness tester. Hardness value obtained in HV scale and 10 points readings were taken along horizontal axis on polished surface. The test was carried out in the micro-forces range under a load of 200 gmf and a dwell time of 15 Seconds. The Vickers microhardness tester which was used **Make: LECO**

Corporation, Michigan, USA, Model: LM-248AT, Ser No XM8116, Date: 02-2013) with 50X magnification. Vickers hardness value HV was obtained directly on the display screen by measuring Diagonal of Diamond point indentation D_1 & D_2 . The picture of the machine are shown below:



Figure 8: Microhardness Testing machine

4.7 Cutting of Sample:

For the purpose of Scanning Electron Microscopy, X-ray Diffraction and corrosion Test, the samples of dimension length x width x thickness (25mm x 10 mm x 5 mm) were further cut off in two part of dimension 12.5 mm x 10 mm x 5 mm each by using the Struers Secotom-20 mounted an abrasive silicon carbide cutting wheel (0.5 mm thick, 200 mm dia). Cutting edges and burr were removed by polishing mechanically with emery paper.



Figure 9: Sample Cutting (12.5 x 10 x 5 mm)

4.8 SEM & EDX (Scanning Electron Microscopy and Energy Dispersive Spectroscopy):

Metallographic phase analysis and chemical characterization/elemental analysis of base sample and the four Age hardened samples were obtained by HITACHI SU 3800 Scanning Electron Microscope under secondary electron imaging mode in FESEM.



Figure 10: Scanning Electron Microscope

4.9 X-Ray Diffraction (XRD):

X-ray Diffraction was carried out to study diffraction pattern and crystallographic phases analysis of the samples in an X-ray diffractometer (Rigaku SmartLab Japan), model Ultima III, 40 KV, 30 mamp (1.2 KW) equipped with Smart Studio II software. XRD instrument was configured with the required measuring parameters, such as copper beam target wavelength 1.5406 \AA , scanning range of 10° to 100° and the scanning rate of 2 degree/min.



Figure 11: XRD Machine

4.10 Corrosion Test:

Corrosion tests were carried out to determine how susceptible to localized corrosion attack of the sample to create a crack or pit and its ability to create a passive layer by alloying elements in corrosive environments. The purpose of the test was to assess the corrosion resistance of the material and its applicability in salt and acidic medium. The study was conducted utilizing an electrochemical approach known as linear polarization resistance. The corrosion potential of the alloys under investigation was examined using the open circuit potential transient technique. Potentiodynamic polarization measurement was used to determine the corrosion parameters, such as corrosion potential (E_{corr}), corrosion current (I_{corr}), corrosion rate in mm/year that is material loss due to corrosion in real time and the capacity of alloys to form the passive layer. Corrosion behaviour of 6063 Al alloy was studied by Tafel polarization techniques and electrochemical impedance spectroscopy (EIS) by Autolab.

For this purpose electrochemical measurements were conducted on five samples which were subjected to the usual metallographic polishing before they were tested. Potentiodynamic linear polarization tests were carried out in a potentiostat by using three electrodes, with the specimen acting as the anode, a graphite rod working as the counter electrode and a saturated calomel electrode (SCE) acting as the reference electrode with respect to which the potential values were measured. The specimen were carefully suspended in two medium like **3.5 wt% NaCl solution and 0.1M H₂SO₄ solution** which acted as an electrolyte. Only the area at cross-section remained exposed whereas the rest of the specimen was carefully wrapped in Teflon tape in order to prevent any current contribution from the adjacent areas. The tests were performed at a scan rate of 0.001 Vs^{-1} over scan range of -0.7V to 1V, starting from the OCP (Open Circuit Potential) values that were measured after 10 min. External overvoltage was impressed upon the circuit from which the corresponding current (i_{app}) was recorded as the difference between anodic and cathodic currents. The characteristic active-passive polarization curves were obtained and the E_{corr} , I_{corr} values were established by using the coordinates of the intersection point of the linear cathodic and anodic branches of the curve. Equipment used MULTIAUTOLAB M204, Model: MAC90833, 13/01/2022, 700VA, 50/60 Hz; MAKE Metrohm Autolab, Netherland. The machine was coupled computerized software NOVA.

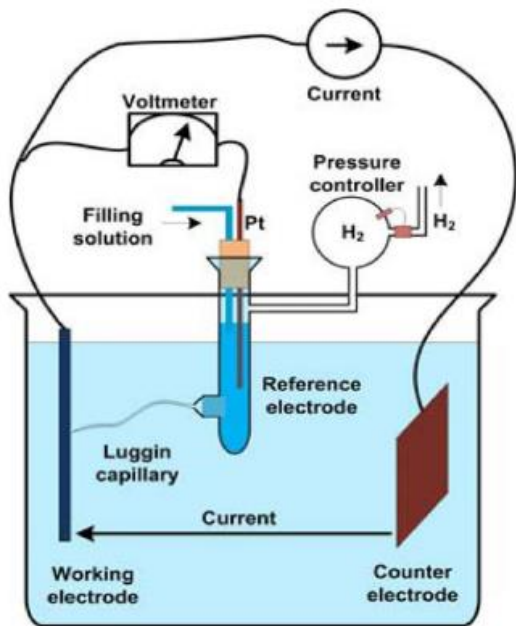


Figure 12: Circuit Diagram of corrosion Test



Figure 13: Corrosion Testing Autolab instrument

CHAPTER - 5

• RESULTS AND DISCUSSION

5.0 Result and Discussion:

5.1 Chemical Composition:

Chemical Compositions of the Al-Alloy AA 6063 was obtained by spectroscopic analysis as shown in **Table: 4:**

Table: 4 Chemical Composition of Base Material

Cu %	Fe %	Si%	Ni%	Zn%	Mg %	Mn %	Ti%	Cr %	Pb %	Sn %	Al %
0.004	0.18	0.412	0.0085	0.0018	0.465	0.053	0.0013	0.001	0.044	0.014	98.8

From the above result it was observed that major alloying element Si and Mg 0.412 and 0.465 in wt % present respectively in Al alloy 6063. Iron (Fe) present 0.18% as an impurities and rest are Al. Other elements composition like Cu, Ni, Zn, Mn, Ti, Cr, Pb and Sn were found insignificant.

5.2 Microstructure observed using an optical microscope:

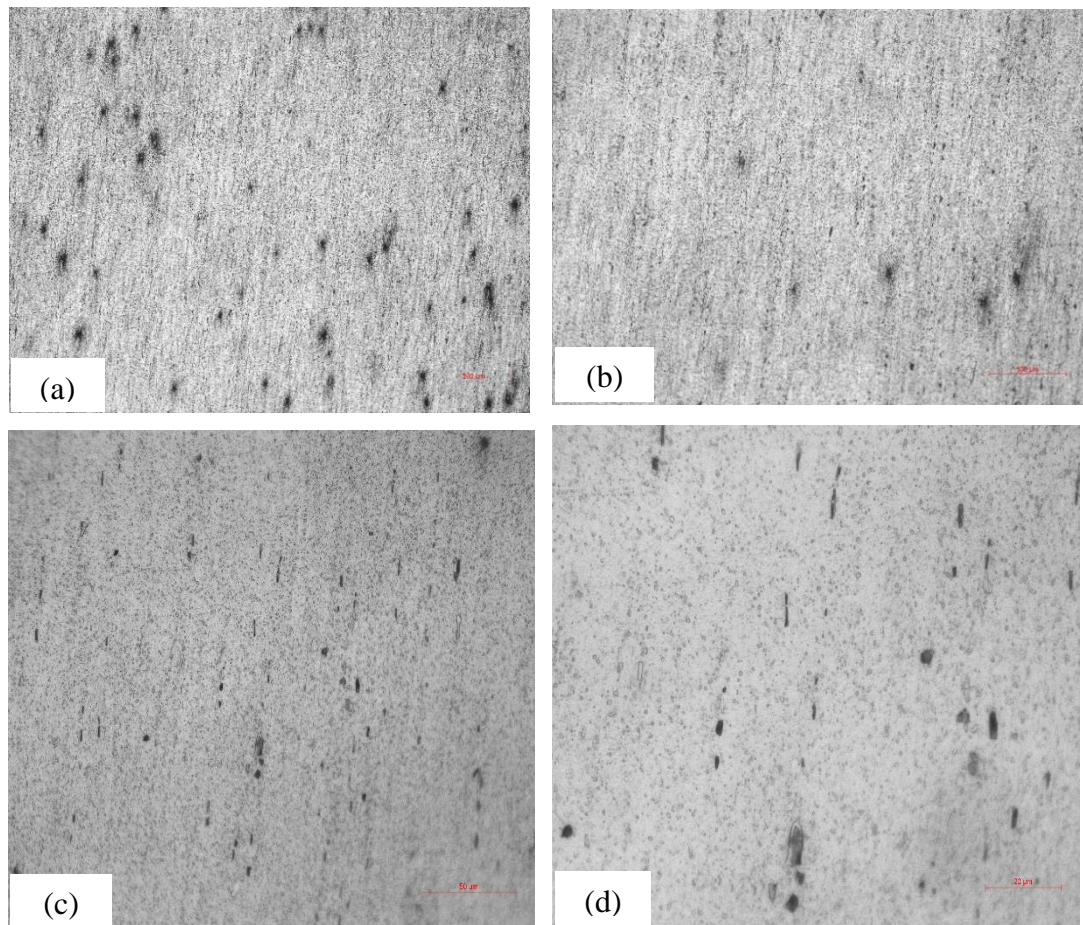


Figure 14: Microstructure of Base sample (a)10x, (b)20x, (c)50x, (d)100x

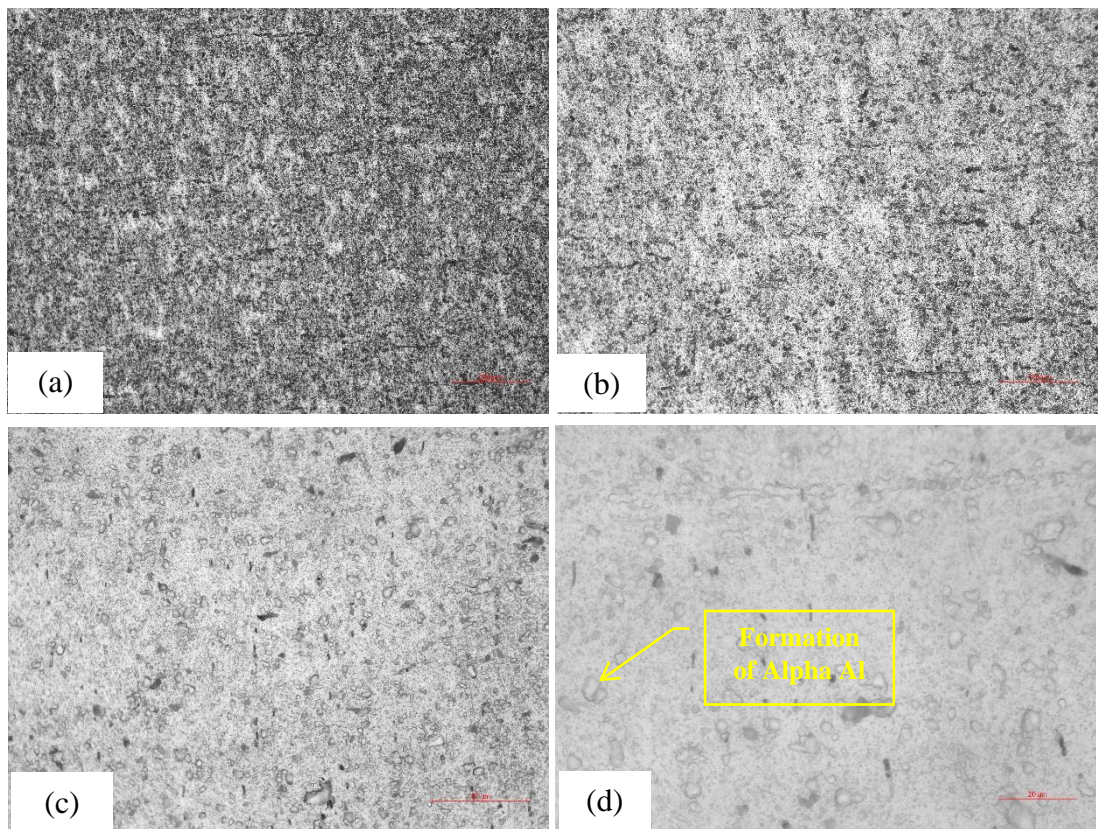


Figure 15: Microstructure of 120°C, 2hrs sample (a)10x, (b)20x, (c)50x, (d)100x

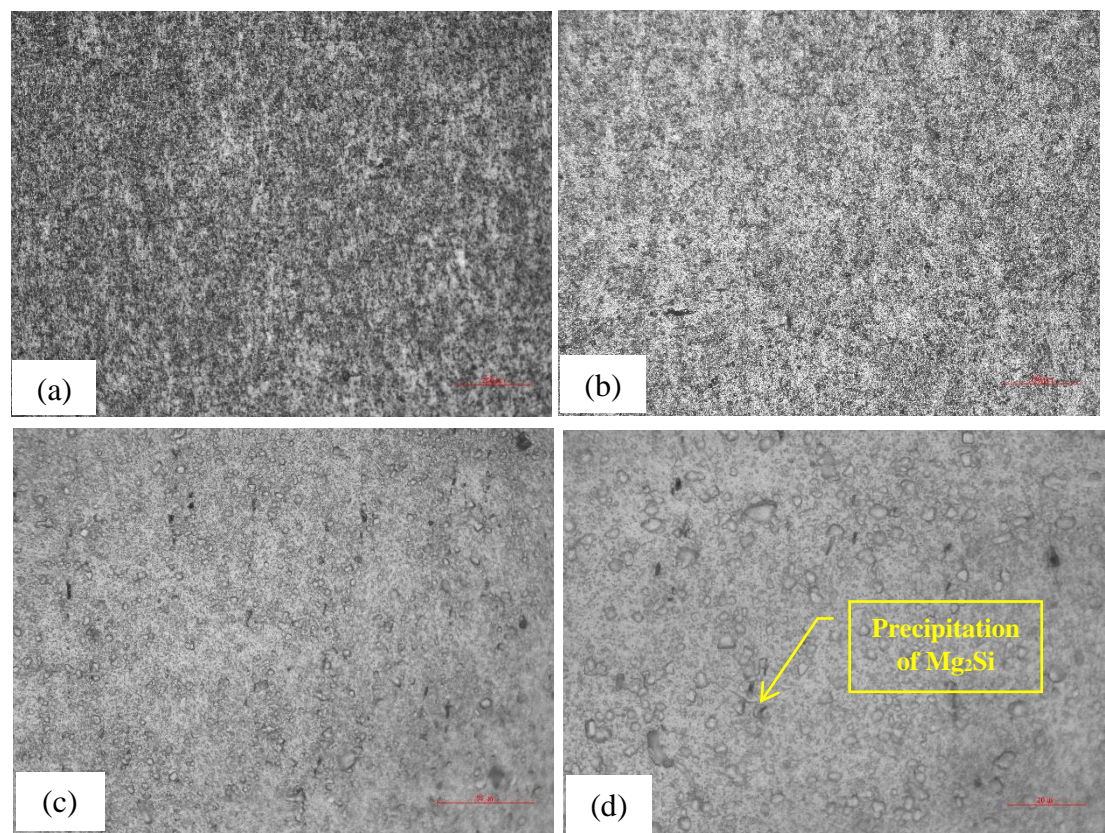


Figure 16: Microstructure of 170°C, 2hrs sample (a)10x, (b)20x, (c)50x, (d)100x

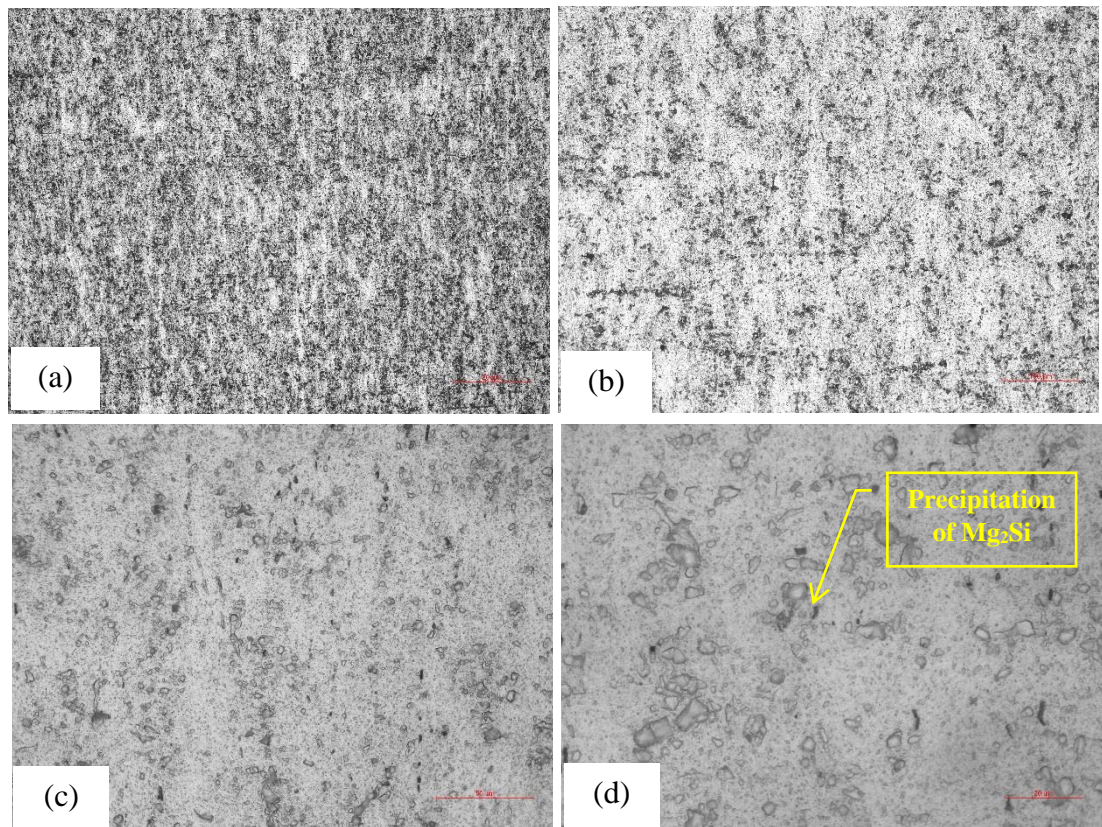


Figure 17: Microstructure of 220°C, 2hrs sample (a)10x, (b)20x, (c)50x, (d)100x

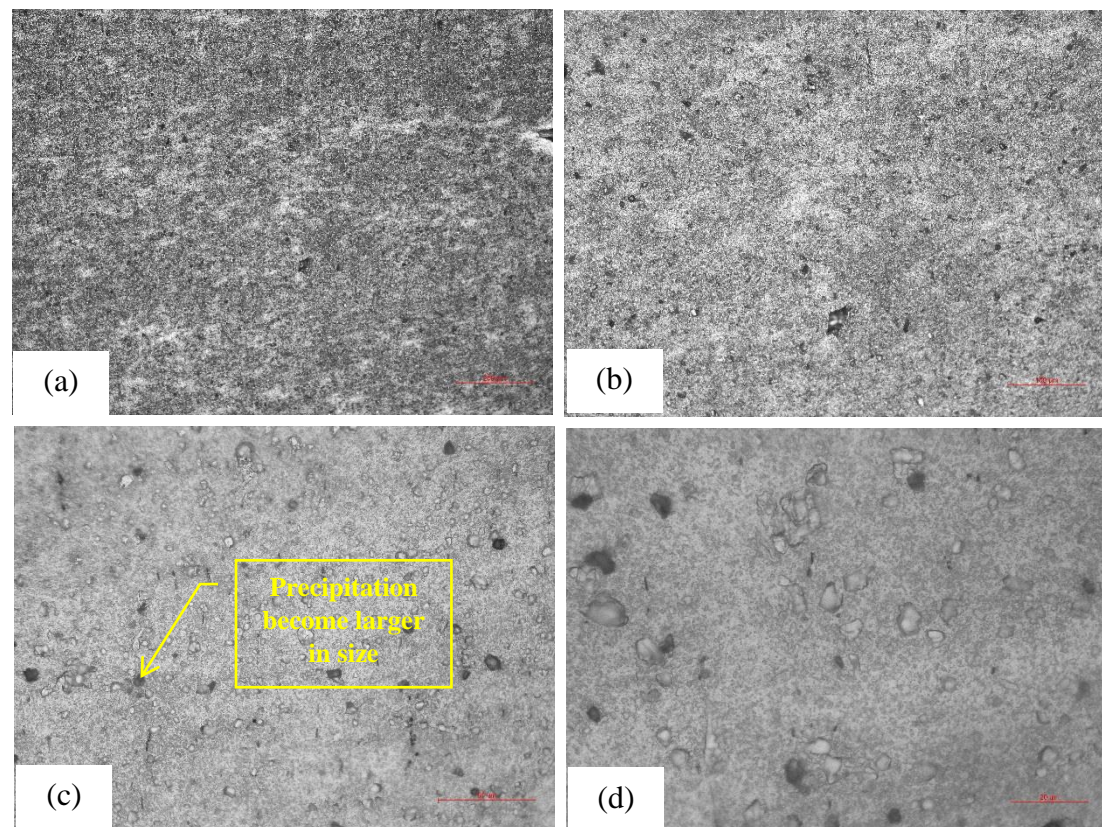


Figure 18: Microstructure of 250°C, 2hrs sample (a)10x, (b)20x, (c)50x, (d)100x

The five specimens of Al 6063 alloy (one Base sample, four age hardened 120°C, 170°C, 220°C and 250°C sample) were subjected to analysis of microstructure in optical

microscope. Proper polishing and etching were carried out before microscopic examination. A metallurgical optical microscope with accessories was used for capturing the images using lens with magnification of 10x, 20x, 50x & 100x for analysis of microstructure.

The microstructure obtained has shown in sub-para 5.2 figure 14 to 18, which reveal change in microstructure in all five samples. In case of base sample it was found small Si flakes distributed in aluminium matrix, however formation of silvery-whitish in appearance uneven shape and size inhomogeneous clustering microstructure were found in case of 120°C, 170°C, 220°C and 250°C sample. The size of cluster were found gradually fine to coarse structure with increasing in temperature.

During precipitation transformation of Al-Cu system phase diagram, Alpha supersaturated Al transform into Alpha saturated Al and θ as a precipitate of intermetallic compound when cooling from solidus temperature to tie line of solvus temperature that also depends on cooling rate of cooling. In case of age hardening process optimization of two parameters, aging temperature and ageing period are necessary to control rate of precipitation nucleation and growth to get reasonable properties. [1] In many previous research papers ascertained that when age hardening begun, both magnesium and silicon began to separate from the solid solution and precipitate as Mg_2Si and other intermetallic compound. Early precipitation was entirely consistent with the Al matrix. [14]

In this analysis also microstructure alteration was observed with the aging treatment and intermetallic precipitates in the structure dispersed finely. Analysis of the surface morphology was done with field emission scanning electron microscopy (FESEM) and an energy dispersive X-ray spectroscopy (EDX) result has been shown in this chapter subsequent para 5.4 and 5.5. In FESEM micrographs with magnification upto 3000x, also ascertained formation of cluster in case of age hardened samples which are disperse uneven manner in the matrix.

One important observation was made in this present study, in EDS spectrum elemental analysis only Al peak with wt% ranging from 96.69 to 97.17 and Mg wt% were 2.03 to 2.19 and Si 0.78 to 1.16%, there was no any intermetallic compound (Mg_2Si) precipitates. In XRD analysis also support the same statement that in four different crystallographic plane only Al peaks were observed except only one intermetallic compound ($Mg_6Si_7Cu_{16}$) peak was found of the sample aging at temperature 220°C for 2 hours duration, there were Mg, Si, Mg_2Si peak were absent. Therefore phase transformation and formation of intermetallic precipitation not fully occurred with this set of age hardening process parameters (temperature and time). So, silvery-whitish clusters which were formed on the surface of age-hardened samples can be identified as **unsaturated α -Al and less amount of intermetallic compounds of Al-Mg-Si-Cu were traced.**

5.3 Microhardness Data in HV scale, Load: 200gf, Dwell Time 15 sec:

Table: 5 Microhardness Data in HV scale of base sample

Sample	Points	D ₁ in μm	D ₂ in μm	HV	Range (Max-Min) HV
Base	i)	63.20	63.2	91.6	$(92.5 - 82) = 10.5$
	ii)	63.64	70.87	82.0	
	iii)	63.06	67.86	86.6	
	iv)	62.68	64.76	91.4	
	v)	61.75	65.20	92.1	
	vi)	63.01	63.66	92.5	
	vii)	64.83	64.83	88.2	
	viii)	64.58	65.62	87.5	
	ix)	65.43	65.43	86.6	
	x)	64.78	65.44	87.5	
Average		63.696	65.687	88.6	

Table: 6 Microhardness Data in HV scale of sample 120°C, 2 hrs

Sample	Points	D ₁ in μm	D ₂ in μm	HV	Range (Max-Min) HV
120°C, 2 hrs	i)	74.87	75.56	65.6	$(76.6 - 65.6) = 11$
	ii)	74.24	73.31	68.1	
	iii)	72.22	71.98	71.3	
	iv)	71.88	74.21	69.2	
	v)	71.62	71.62	72.3	
	vi)	66.4	74.57	74.7	
	vii)	66.56	72.58	76.6	
	viii)	71.53	71.39	72.6	
	ix)	72.34	72.34	70.9	
	x)	71.07	73.36	71.1	
Average		71.273	73.092	71.24	

Table: 7 Microhardness Data in HV scale of sample 170°C, 2 hrs

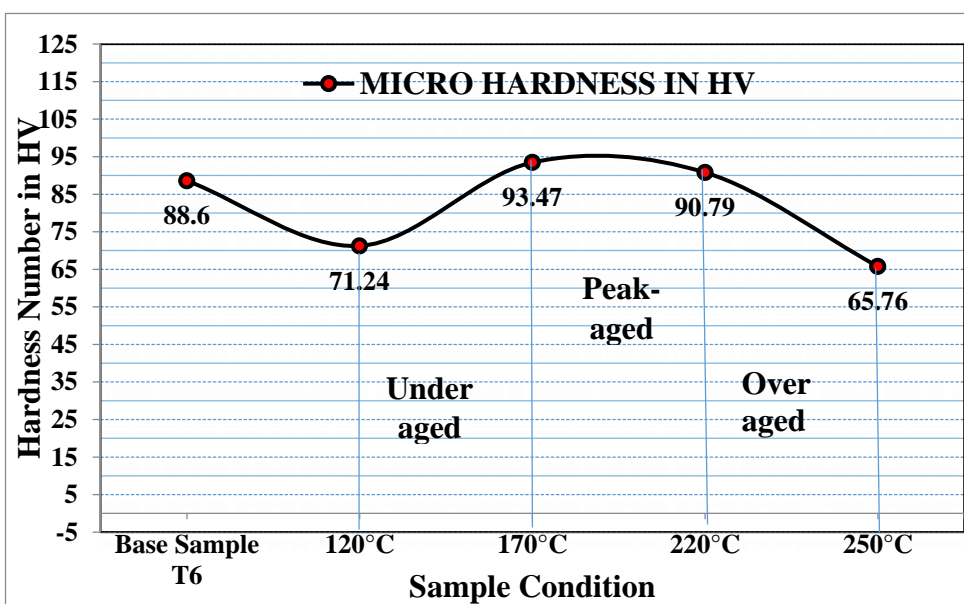
Sample	Points	D ₁ in μm	D ₂ in μm	HV	Range (Max-Min) HV
170°C, 2 hrs	i)	62.85	64.17	91.9	$(100.6 - 86.1) = 14.5$
	ii)	64.97	66.26	86.1	
	iii)	62.96	64.85	90.8	
	iv)	63.38	65.75	88.6	
	v)	63.88	64.98	89.3	
	vi)	60.02	61.81	100	
	vii)	61.12	63.97	94.8	
	viii)	60.37	61.06	100.6	
	ix)	61.96	63.90	93.7	
	x)	60.61	61.86	98.9	
Average		62.212	63.861	93.47	

Table: 8 Microhardness Data in HV scale of sample 220°C, 2 hrs

Sample	Points	D ₁ in μm	D ₂ in μm	HV	Range (Max-Min) HV
220°C, 2 hrs	i)	67.11	67.15	82.3	$(93.7 - 82.3) = 11.4$
	ii)	63.00	63.43	92.8	
	iii)	63.49	63.49	92.0	
	iv)	63.54	63.54	91.9	
	v)	61.42	64.38	93.7	
	vi)	63.29	64.99	90.2	
	vii)	63.23	64.22	89.9	
	viii)	62.86	63.83	92.4	
	ix)	63.88	64.35	90.2	
	x)	63.31	63.31	92.5	
	Average	63.513	64.269	90.79	

Table: 9 Microhardness Data in HV scale of sample 250°C, 2 hrs

Sample	Points	D ₁ in μm	D ₂ in μm	HV	Range (Max-Min) HV
250°C, 2 hrs	i)	76.65	76.65	63.10	$(70.1 - 62.3) = 7.8$
	ii)	74.71	76.24	65.1	
	iii)	75.42	78.60	62.5	
	iv)	74.85	79.41	62.3	
	v)	74.16	74.16	67.4	
	vi)	74.26	75.20	66.4	
	vii)	74.35	74.50	67.0	
	viii)	74.57	75.26	66.10	
	ix)	72.75	72.75	70.10	
	x)	74.06	74.12	67.6	
	Average	74.578	75.689	65.76	

**Figure 19: Graphical Representation of Average Microhardness Value (five samples)**

The ageing response of five samples (base and four age-harden sample) were studied based on the evolution of micro hardness in HV scale, result is shown in sub-para 5.3 and figure 19. Average ten points hardness value were 88.6, 71.4, 93.47, 90.79 and 65.76 HV for the base sample, age hardened sample of 120°C, 2 hrs, 170°C, 2 hrs, 220°C, 2 hrs and 250°C, 2 hrs respectively. Maximum hardness value reached upto 100 HV at 170°C, 2 hrs, this is referred to as peak-aging (PA) state. The peak hardness value obtained in this study is in close agreement with previous researcher Aluru Praveen Sekhar*, Debdulal Das [8], reported peak hardness value reached upto 98 ± 0.75 HV_{2.0} for similar Al-Mg-Si alloy aged at 150 °C with aging period 120 h. Another Authors Ahmet Meyvecia , Ismail Karacana , Ugur C, aligülü b , HülyaDurmus, c,*[11] also obtained highest hardness values of AA 6063 Al alloys were 100 HV when the samples were aged at 180°C.

In present study Hardness value observed during ageing at 120°C period 71.24 HV was identified as under-aged (UA) condition. Hardness value decreased from 90.79 HV to 65.76 HV while ageing temperature increased from 220°C to 250°C. Therefore 250°C was identified as Over-aged (OA) condition.

It was observed hardness value gradually increasing and decreasing over a temperature range from 120°C to 250°C, can be explained by the following reasons:

i) One aspect may be emphasized, during PA state fine distribution of coherent precipitation of second phases (Mg₂Si) in the Al matrix. Precipitation act as an obstacle to dislocation motion and the driving force is interfacial energy between precipitate and Al matrix. When precipitations are fine and coherent extra energy needed to move dislocation through slip plane resulting increase in hardness value.

In UA condition, precipitation density is less as formation of precipitation is stage of starting and OA condition fine distribution of precipitate change into coarse distribution with larger in size, less obstacle to dislocation movement resulted decrease in hardness.

ii) Second aspect may be due to uneven shape and size inhomogeneous distribution clustering microstructure which was observed in optical microscope (sub-para 5.2, Figure 14 to 18) and SEM micrographs (sub-para 5.4, Figure 20 to 24) also reveal the same. Increment in hardness due to lattice mismatch caused by the formation of a higher volume fraction of formation of Guiner and Preston (GP zones) which disturbs the regularity in the lattice. The clustering may produce local strain around them which acts as obstacles to the easy movement of dislocation, so that the hardness of GP is higher than for the solid solution.

5.4 FESEM image of the Base material sample and Age Harden Samples:

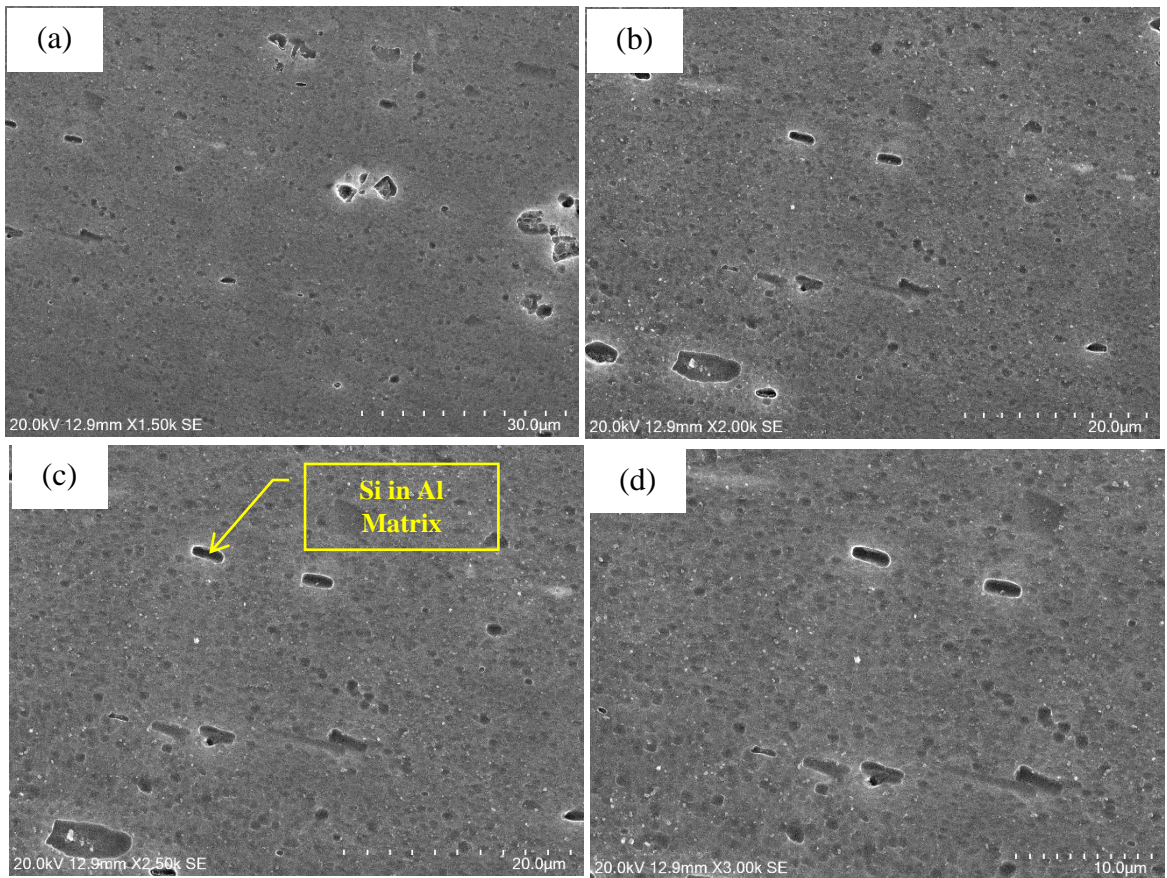


Figure 20: FESEM image of Base Sample (a)1500x, (b)2000x, (c)2500x, (d)3000x

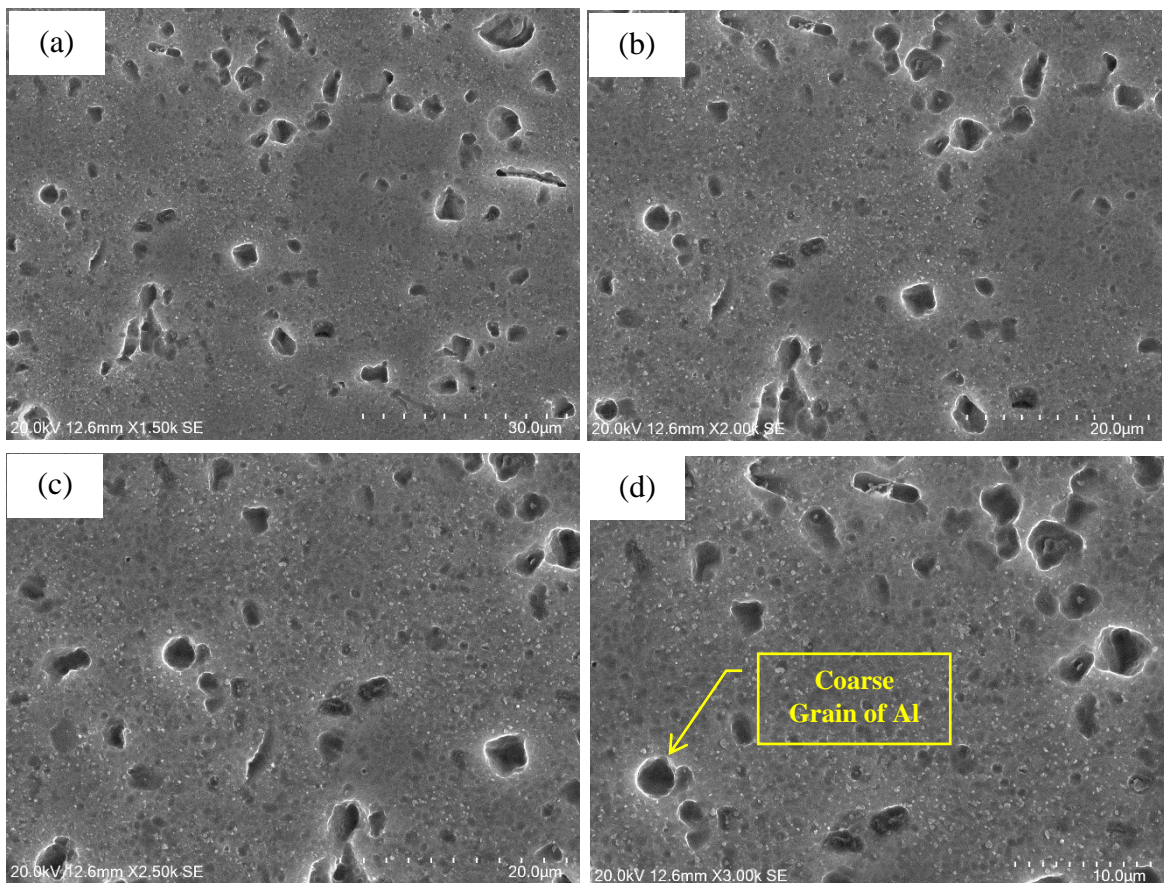


Figure 21: FESEM image of Sample 120°C, 2 hrs duration (a)1500x, (b)2000x, (c)2500x, (d)3000x

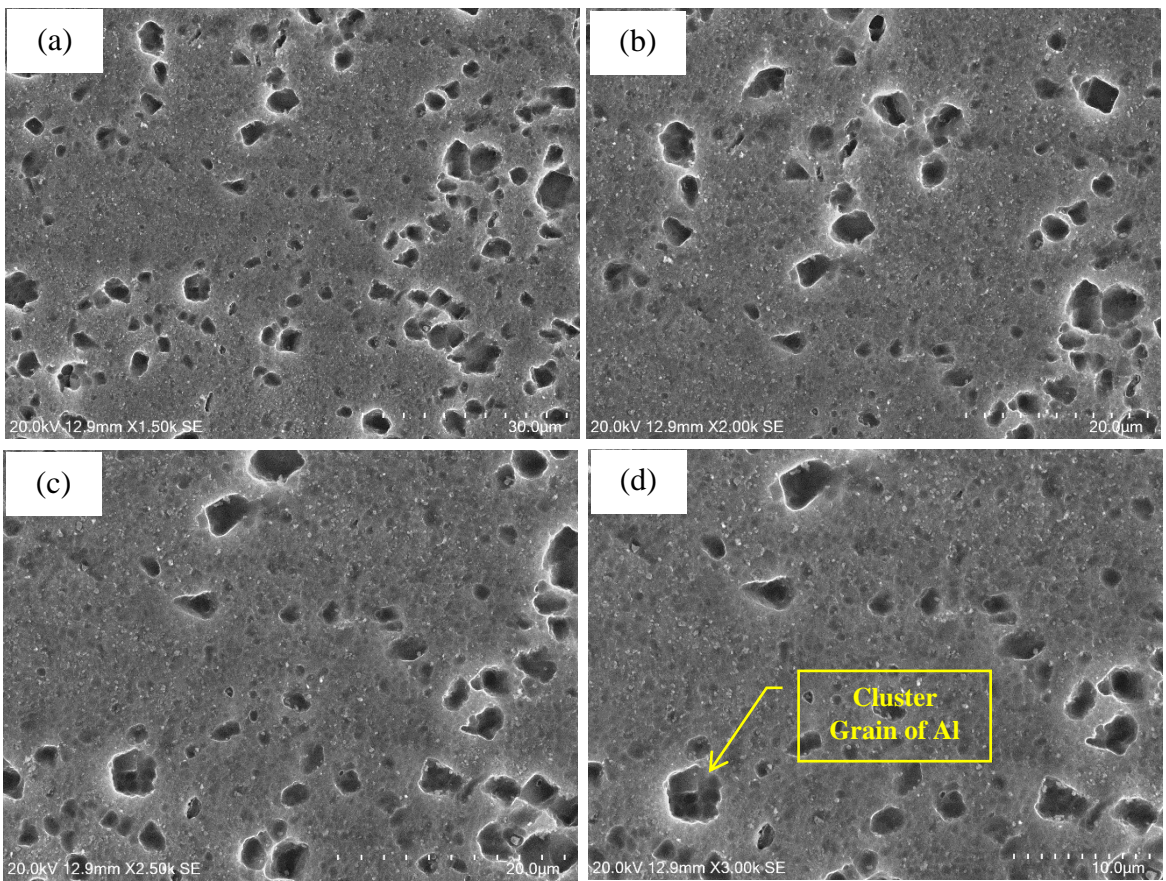


Figure 22: FESEM image of Sample 170°C, 2 hrs duration (a)1500x, (b)2000x, (c)2500x, (d)3000x

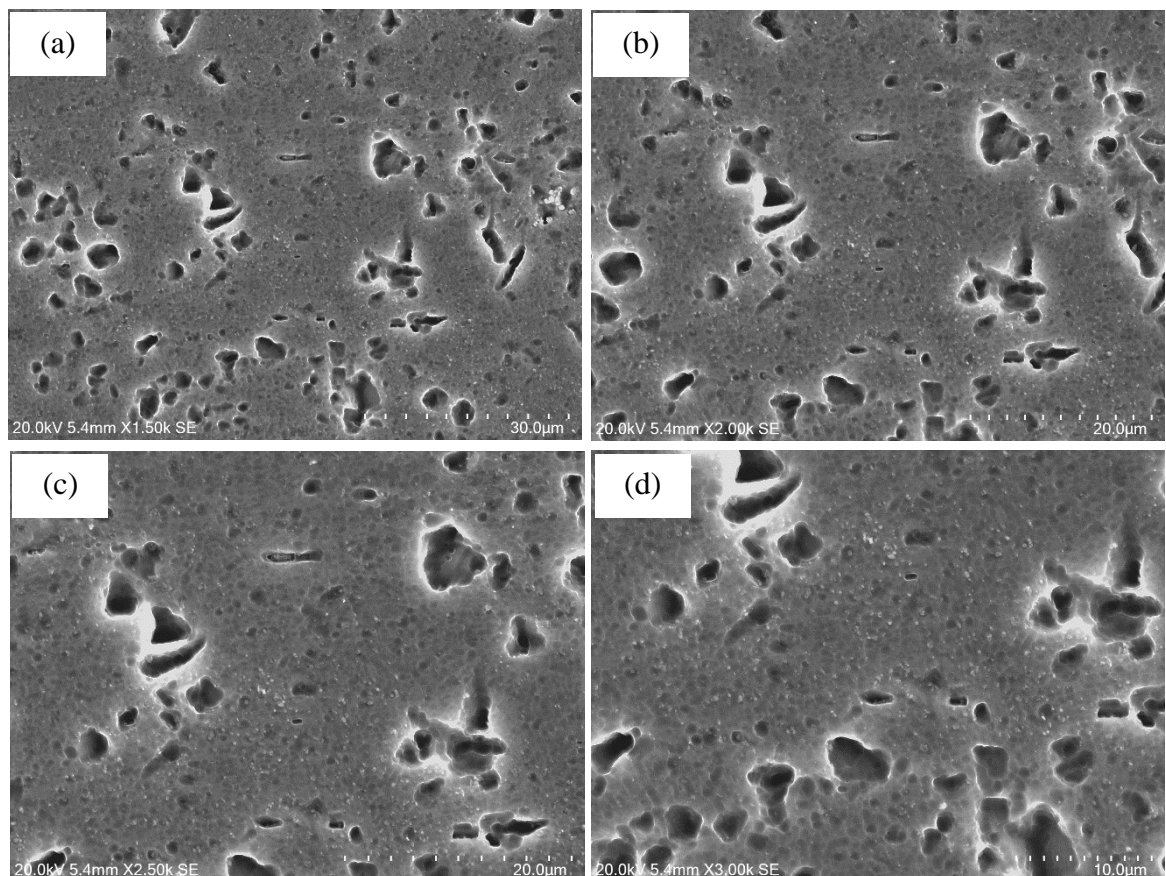


Figure 23: FESEM image of Sample 220°C, 2 hrs duration (a)1500x, (b)2000x, (c)2500x, (d)3000x

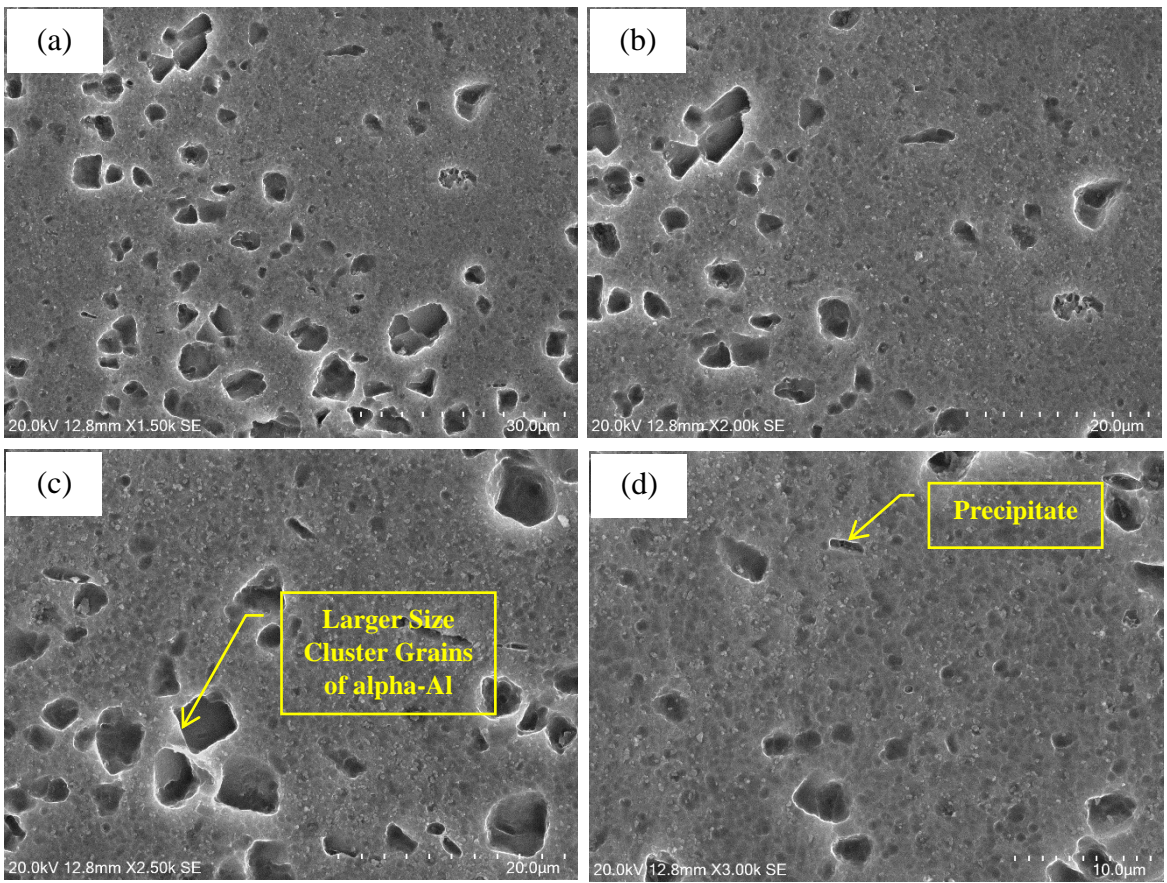


Figure 24: FESEM image of Sample 250°C, 2 hrs duration (a)1500x, (b)2000x, (c)2500x, (d)3000x

The five samples were characterized by using Field Emission scanning Electron microscope (FESEM), before that samples were prepared with suitable method. Micrographs images were captured with four different magnification like 1500x, 2000x, 2500x & 3000x. Base sample and age hardened samples images are shown above in sub para 5.4, figure 20 to 24.

Significant observation was that formation of cluster type micrographs position in different orientation on the surface, were started to form at initial stage of age-hardening process, it was revealed in image of sample artificial age hardening at temperature 120°C, 2hrs. Subsequently its became gradually larger in size and overlapped to each other from temperature range 170°C to 250°C. It has been discussed in detail under sub-para 5.2, wherein formation of α -Al cluster and less amount of intermetallic compounds precipitates of Al-Mg-Si-Cu-Fe into the alloy can be ascertained.

5.5 Energy Dispersive spectroscopy (EDS) result of the Base material and Age-Harden Samples:

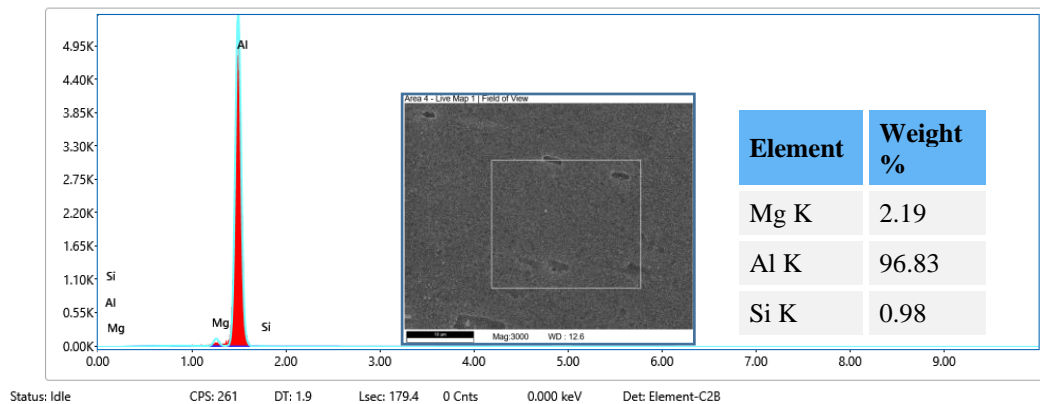


Figure 25: EDS spectrum of Base Sample

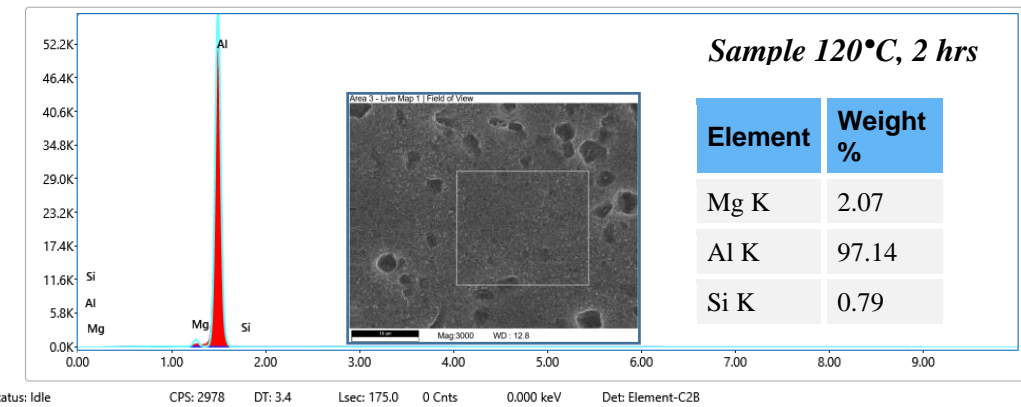


Figure 26: EDS spectrum of Sample 120°C, 2 hrs duration

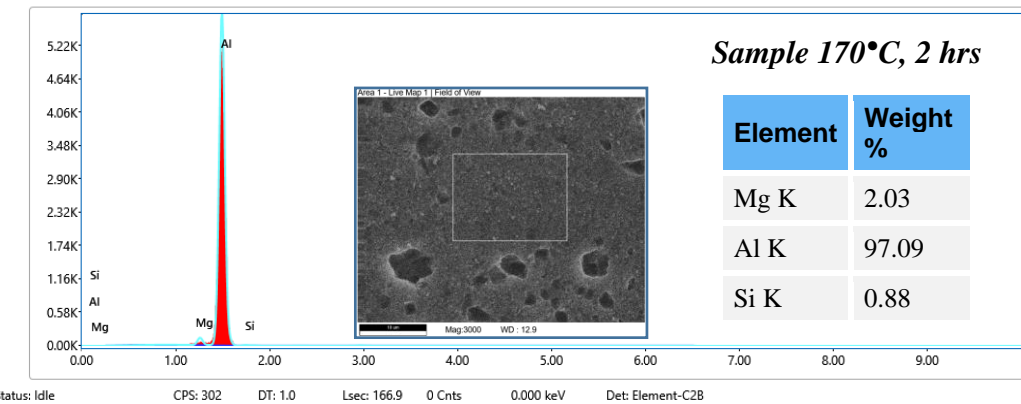


Figure 27: EDS spectrum of Sample 170°C, 2 hrs duration

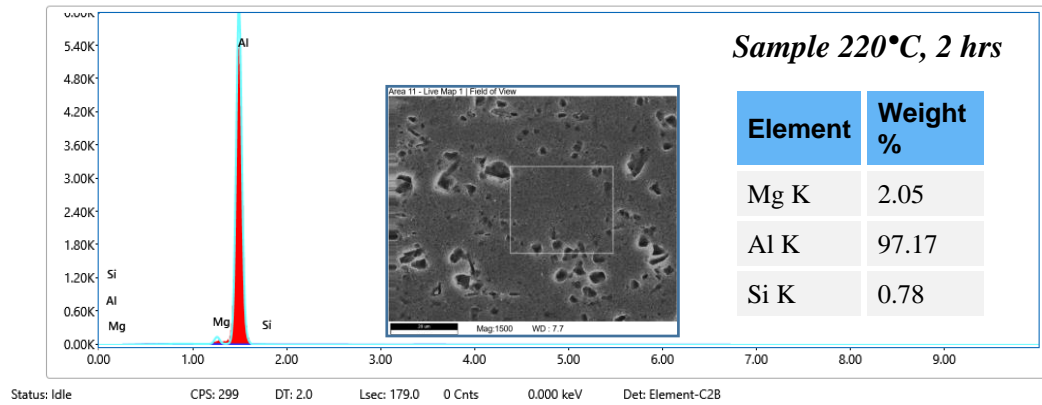


Figure 28: EDS spectrum of Sample 220°C, 2 hrs duration

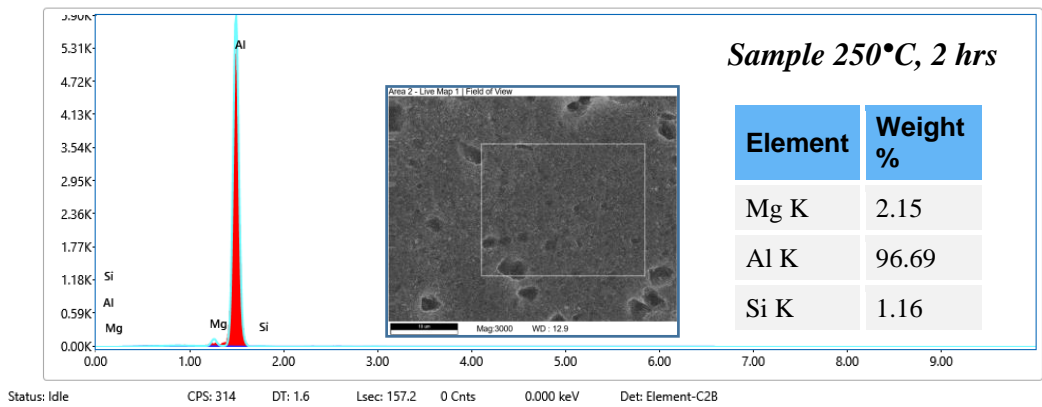


Figure 29: EDS spectrum of Sample 250°C, 2 hrs duration

The five samples were characterized by using Field Emission scanning Electron microscope (FESEM) coupled with Energy Dispersive spectroscopy (EDS), result of Base sample and age hardened samples are shown above in sub para 5.5, figure 25 to 29. Only Aluminium peaks were observed with less percentage of Mg and Si. There were no changes observed with base sample and age hardened sample.

5.6 X-Ray Diffraction (XRD) of the Base material and Age-Harden Samples:

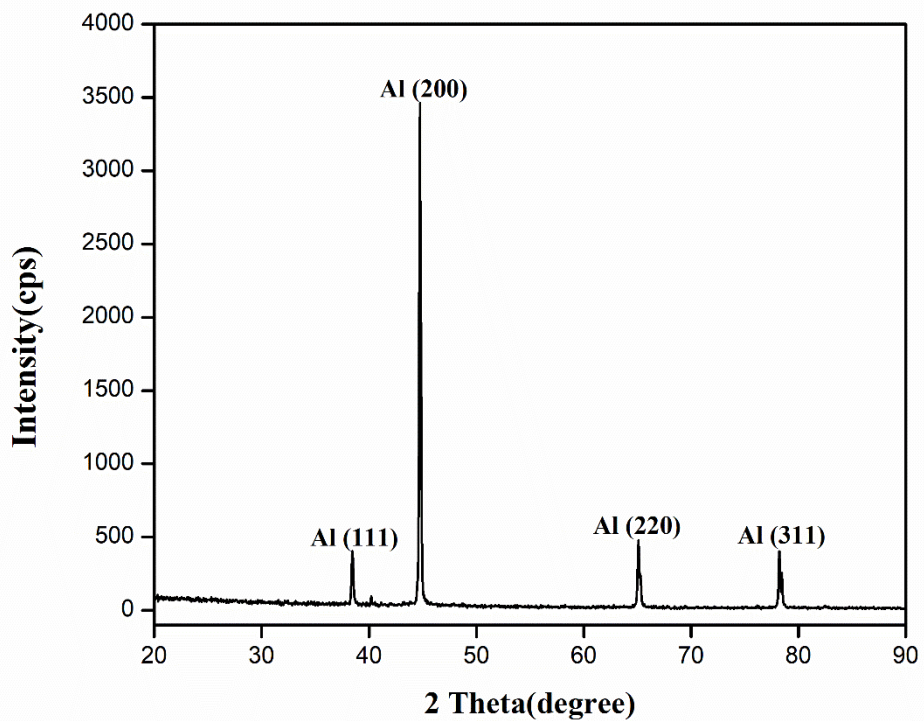


Figure 30: Crystallographic phases of Base Sample

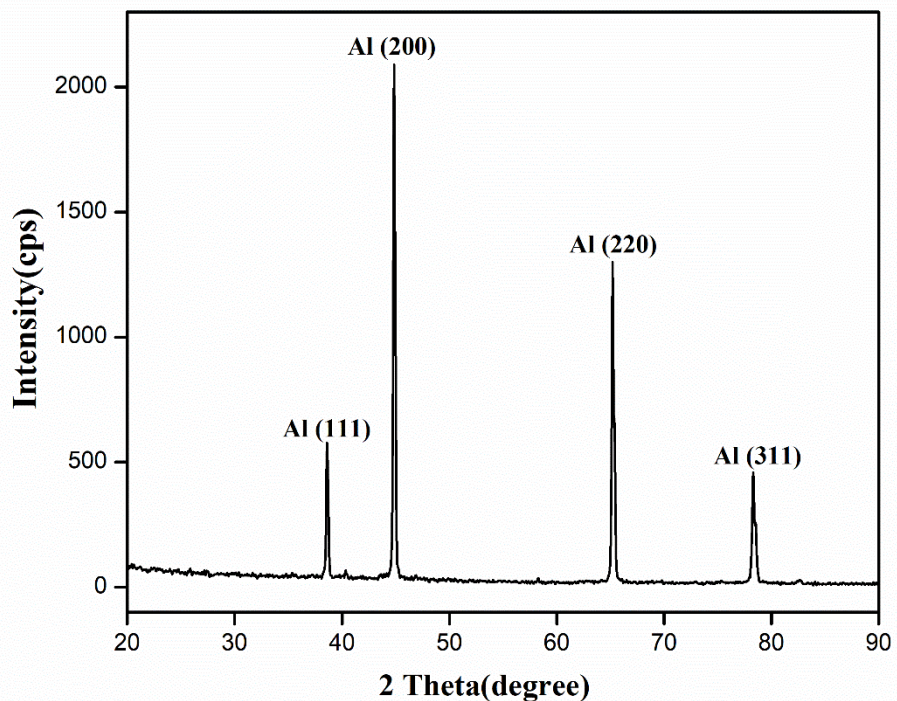


Figure 31: Crystallographic phases of Sample 120°C, 2 hrs duration

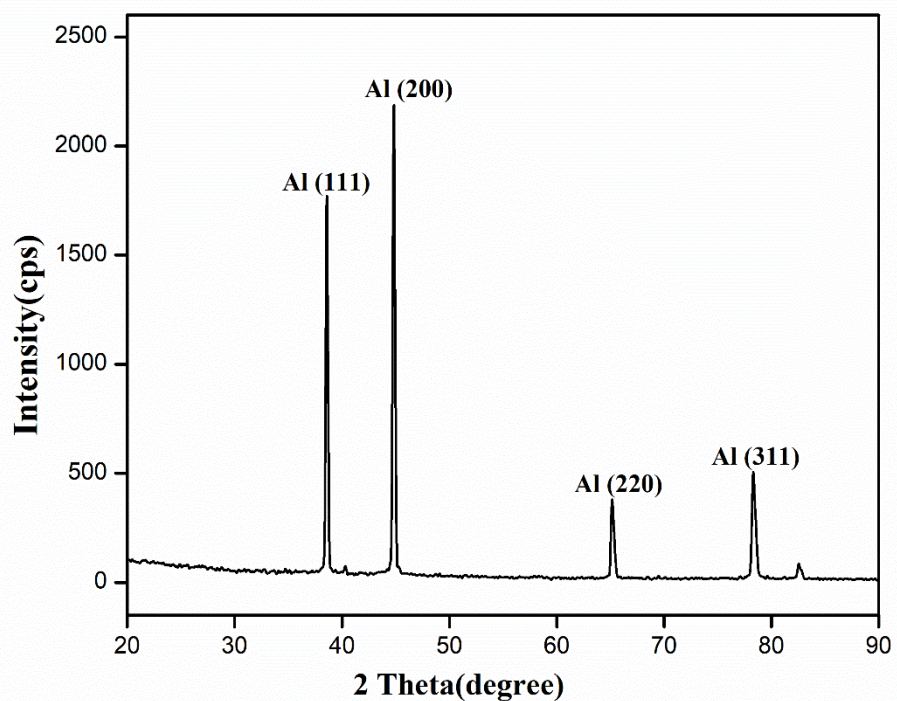


Figure 32: Crystallographic phases of Sample 170°C, 2 hrs duration

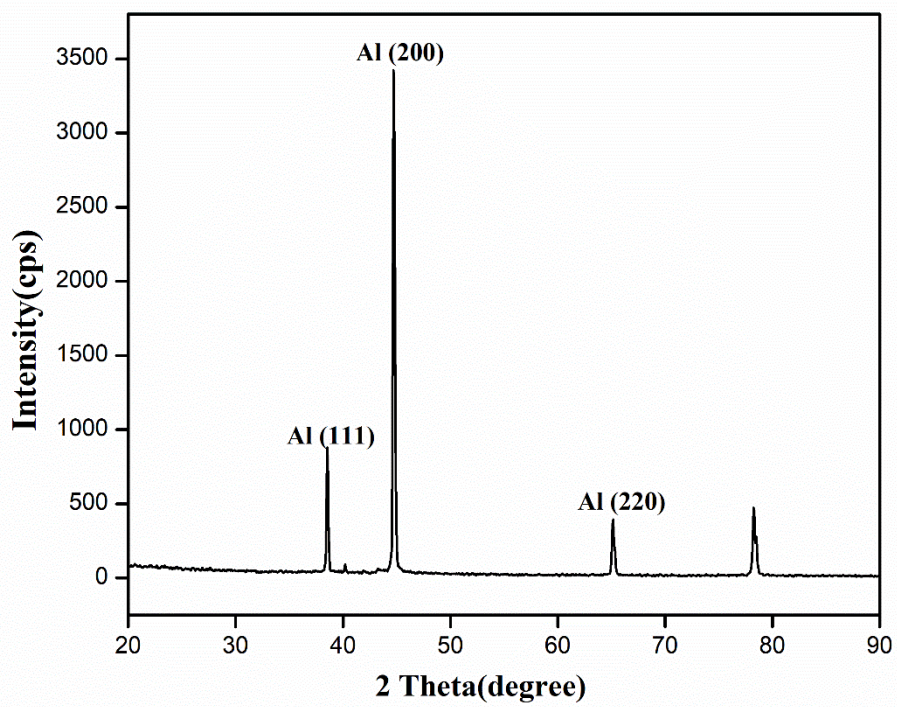


Figure 33: Crystallographic phases of Sample 220°C, 2 hrs duration

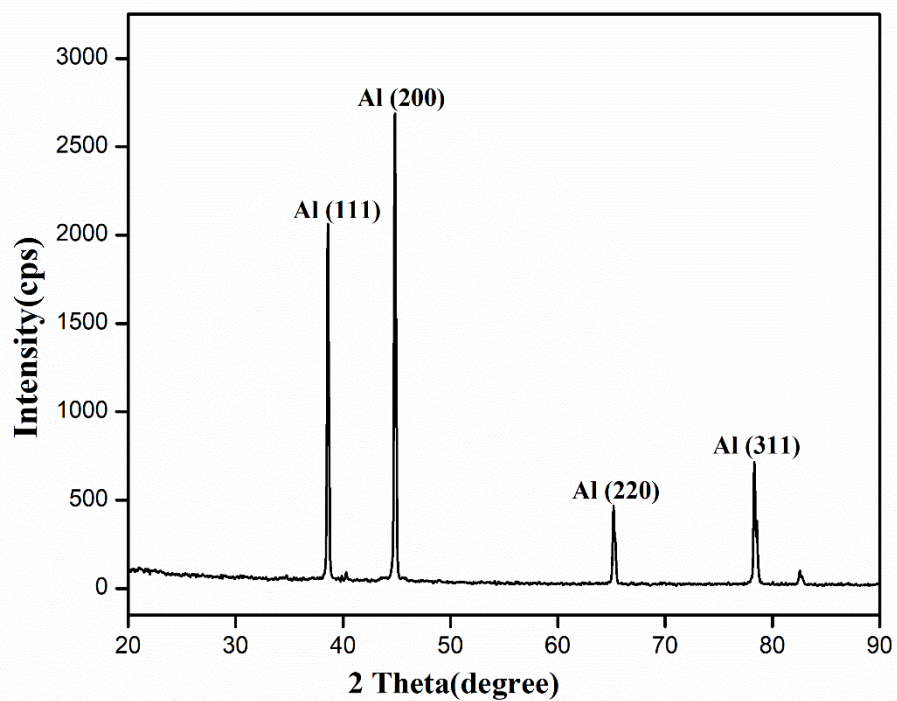


Figure 34: Crystallographic phases of Sample 250°C, 2 hrs duration

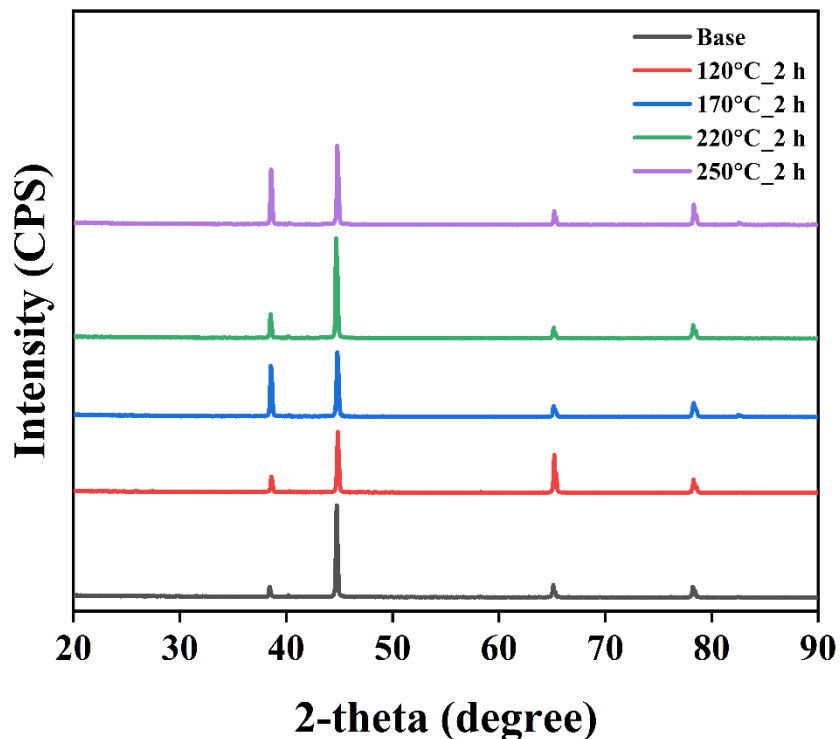


Figure 35: Crystallographic phases of five samples

Crystallographic phase analysis of five samples were carried out by X-ray diffraction technique graphical representation **X-ray intensity (Cycles per Second) vs 2θ in degree** of Base sample and age hardened samples are shown above in sub para 5.6, figure 30 to 35, based

on the result obtained during test by using software, shown in Table 10. All phases were Al except only one intermetallic compound ($Mg_6Si_7Cu_{16}$) peak was found of the sample aging at temperature 220°C for 2 hours duration.

Table: 10 Crystallographic phase analysis by XRD

Sample	Height in %	Phase ID	d (Å)	Intensity %	Plane (hkl)	2θ in °	Delta
Base	10.3	Al	2.3416	100.0	111	38.411	-0.008
	100.0	Al	2.0275	45.4	200	44.689	-0.071
	14.5	Al	1.4330	22.9	220	65.034	-0.056
	12.9	Al	1.2218	22.6	311	78.165	-0.051
120°C; 2 hrs	25.6	Al	2.3322	100.0	111	38.573	-0.002
	100.0	Al	2.0205	45.6	200	44.821	-0.018
	68.9	Al	1.4298	23.2	220	65.197	0.002
	23.7	Al	1.2197	22.9	311	78.331	0.034
170°C; 2 hrs	79.6	Al	2.333	100.0	111	38.553	0.000
	100.0	Al	2.0213	45.6	200	44.801	0.004
	18.7	Al	1.4302	23.2	220	65.177	0.035
	24.3	Al	1.2199	22.9	311	78.311	0.013
220°C; 2 hrs	21.4	Al	2.333	100.0	111	38.554	0.040
	100.0	Al	2.0213	45.5	200	44.803	0.098
	10.6	Al	1.4301	23.3	220	65.180	0.047
	13.9	$Mg_6Si_7Cu_{16}$	1.2213	6.1	931	78.210	-0.044
250°C; 2 hrs	65.7	Al	2.3321	100.0	111	38.574	0.013
	100.0	Al	2.0204	45.5	200	44.823	0.014
	18.3	Al	1.4297	23.3	220	65.200	0.008
	26.9	Al	1.2196	28.8	311	78.334	0.021

5.7 Corrosion Test of the Base material and Age-Harden Samples 3.5 wt% NaCl Solution and 0.1M H₂SO₄ Solution:

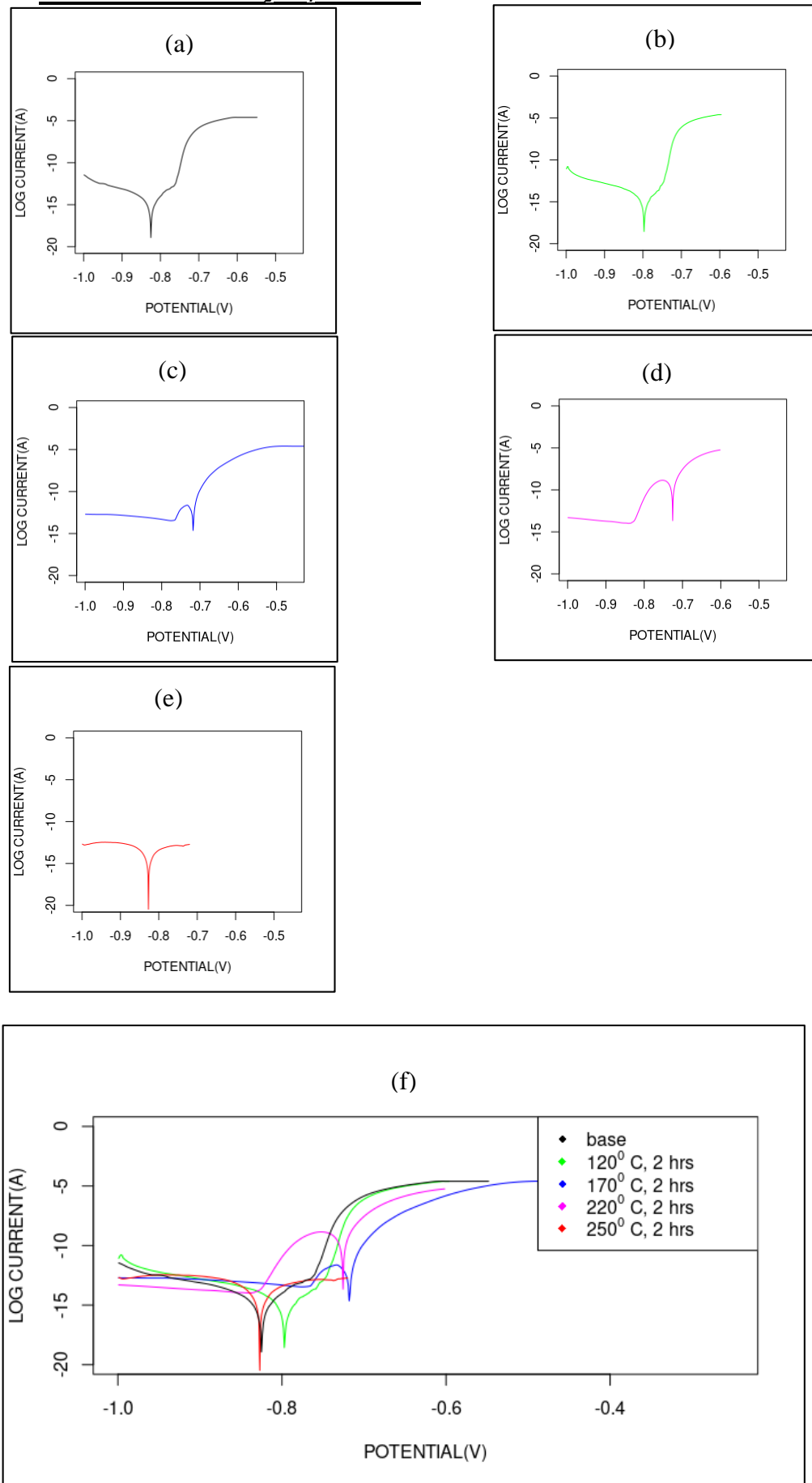


Figure 36: Tafel Plot 3.5 wt% NaCl Solution; Sample (a)base (b)120°C (c)170°C (d)220°C (e) 250°C, 2 hours duration, (f) comparison of five samples

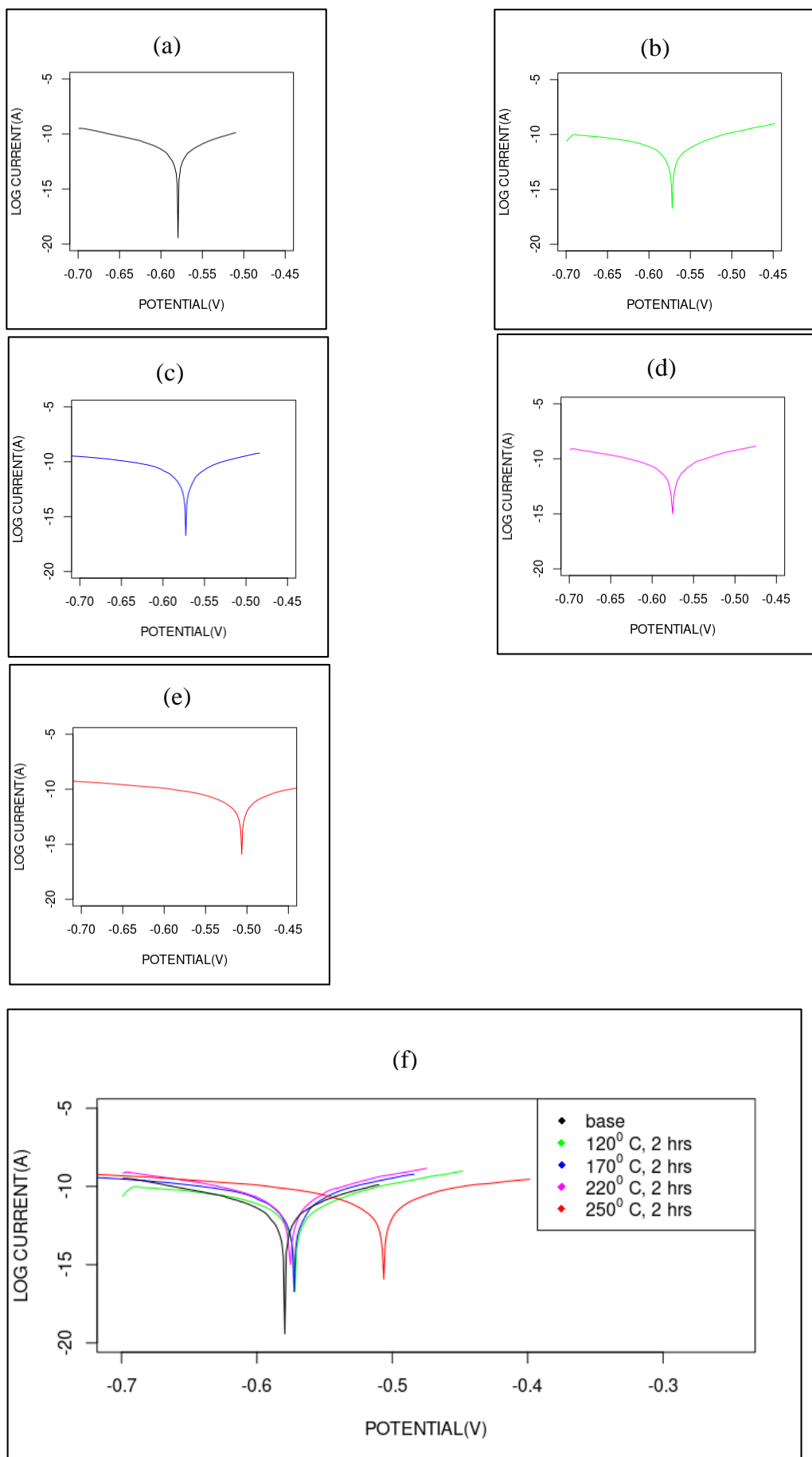


Figure 37: Tafel Plot 0.1M H_2SO_4 Solution; Samples (a)base (b) 120°C (c) 170°C (d) 220°C (e) 250°C , 2 hrs duration, (f) comparison of five samples

5.8 Microstructure study in Optical Microscope after Corrosion Test of the Base material and Age-Harden Samples 3.5 wt% NaCl Solution and 0.1M H₂SO₄ Solution:

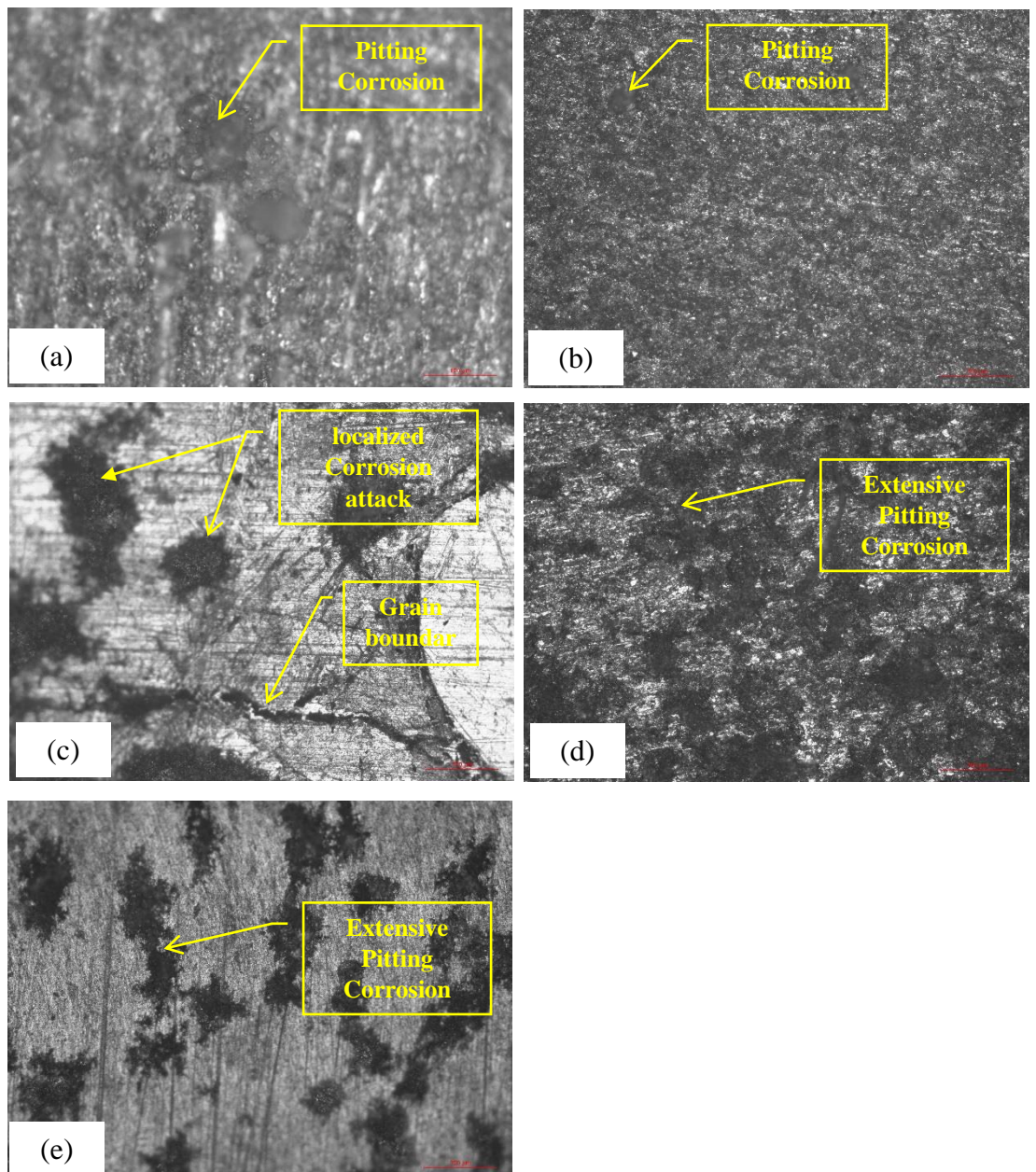


Figure 38: Microstructure after Corrosion test in 3.5% NaCl solution; Samples (a)base sample, 10x (b)120°C/2 hrs, 10x (c)170°C/2 hrs, 10x (d)220°C/2 hrs, 10x (e) 250°C/2 hrs, 10x

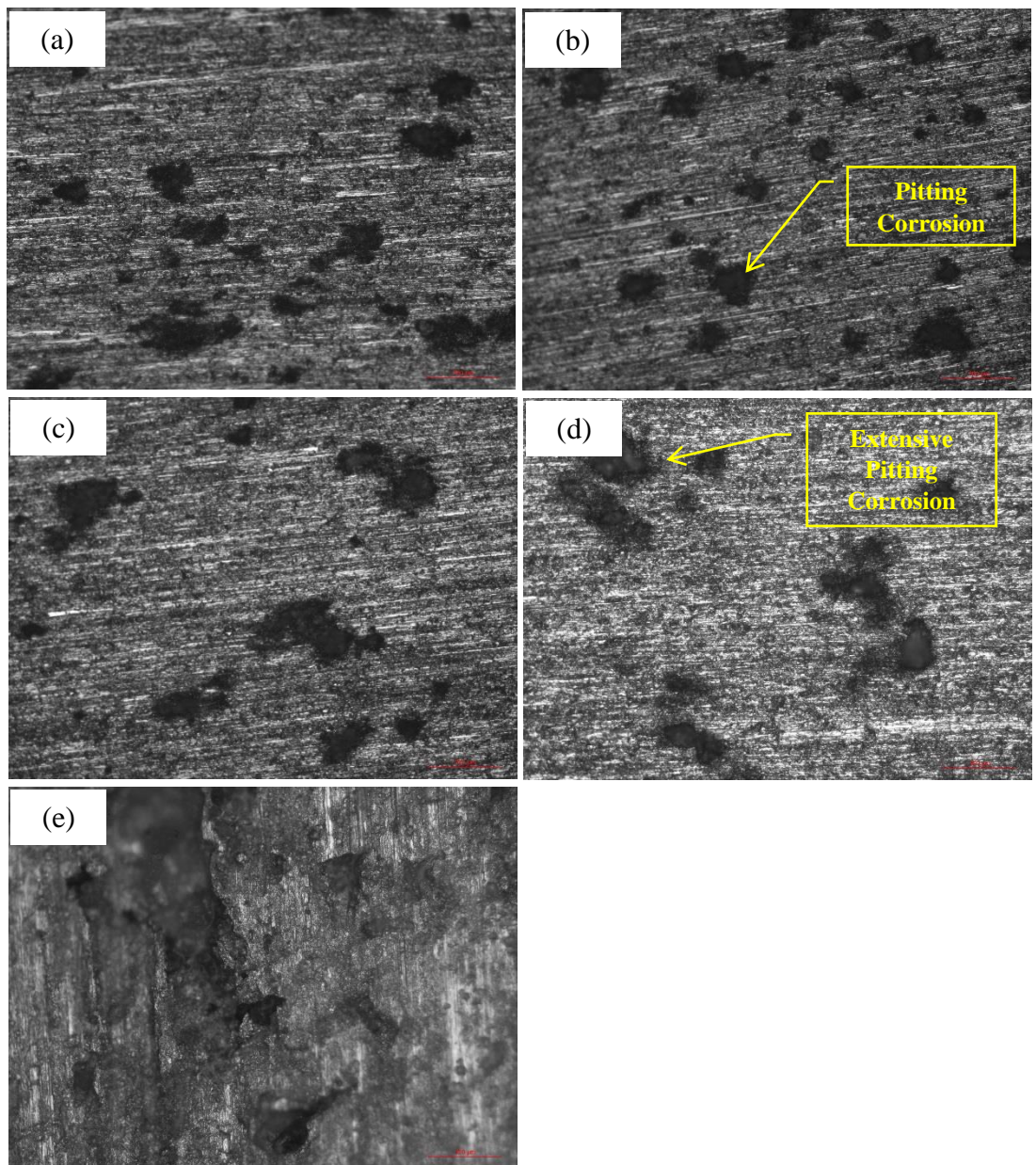


Figure 39: Microstructure after Corrosion test in 0.1M H_2SO_4 solution; Samples
(a)base sample, 10x (b)120°C/2hrs, 10x (c)170°C/2 hrs, 10x (d)220°C/2 hrs, 20x (e) 250°C/2 hrs, 20x

For analysis of corrosion test result and find out corrosion rate of five samples, Tafel polarization techniques was used in Autolab instrument coupled with computerized NOVA software. This is a rapid technique to measure corrosion current and corrosion rate, potentiodynamic anodic polarization is the characterization of a metal specimen by its current potential relationship. Linear Sweep Voltammetry (LSV) plot (logarithmic current (A) vs potential (V) curve) were generated and shown in sub-para 5.7 figure 36, 37 and through extrapolations of the anodic and cathodic linear Tafel region, measure the corrosion current (I_{corr}), Corrosion Potential (E_{corr}), Potential resistance (Z), Tafel Constants slope of the anode and cathode (β_A , β_C) and Rate of corrosion in mm/year. The data and result obtained from the curves are described below:

The empirical formula is used to calculate **corrosion rate (CR)** of the samples:

$$CR = 0.00327 * (a * J_{corr}) / (n * D) \text{ mm/year} \quad [20]$$

Where,

a/n = Equivalent weight of Al-Alloy in gm/mol = 26.981 gm/mol

D = Density of Al-Alloy in gms/cm³ = 2.7 gm/cm³

J_{corr} = Current Density in $\mu\text{amp}/\text{cm}^2$ = $I_{corr}/\text{surface area of the sample exposed to electrolyte}$ [Here surface area of Al-Alloy 6063 sample = $(1.2 * 0.5) = 0.6 \text{ cm}^2$]

Table: 11 Corrosion Parameters in 3.5 wt% NaCl Solution

Sample	Ecorr in (V)	i_{corr} in (μA)	j_{corr} in (μA per cm^2)	Polarization resistance in (Ω)	Tafel Anodic Constant (β_A in V/dec)	Tafel Cathodic Constant (β_C in V/dec)	Corrosion rate in (mm/year)
Base	-0.82582	0.18478	0.30797	45034	0.039082	0.037592	0.010065
120°C, 2hrs	-0.79574	0.15169	0.25282	45520	0.031286	0.032328	0.0082629
170°C, 2hrs	-0.72317	6.1256	10.209	1222.4	0.024494	0.058237	0.33368
220°C, 2hrs	-0.72282	25.011	41.685	266.68	0.02372	0.048985	1.3624
250°C, 2hrs	-0.82535	0.39289	0.65482	21230	0.037036	0.039896	0.021402

From the above data it was found that corrosion rate is lower 0.0082629 mm/year in case of artificial age hardening of Al alloy sample at temperature 120°C with holding time 2 hours and demonstrated a high level of corrosion resistance with its broad passive region and low corrosion current density. In the NaCl salt water solution, al-alloy 6063 at 220°C, 2 hours showed a very high corrosion current density and a short passive zone, indicating limited corrosion resistance. According to the Tafel analysis, the sample corrodes with a relatively high rate and susceptible to localized corrosion attack.

Table: 12 Corrosion Parameters in 0.1M H₂SO₄ Solution

Sample	Ecorr in (V)	i_{corr} in (μA)	j_{corr} in (μA per cm^2)	Polarization resistance in (Ω)	Tafel Anodic Constant (β_A in V/dec)	Tafel Cathodic Constant (β_C in V/dec)	Corrosion rate in (mm/year)
Base	-0.58026	2.17	3.6312	2281.4	0.022643	0.023141	0.11868
120°C, 2hrs	-0.57195	3.926	6.544	2315.5	0.039393	0.044674	0.21388
170°C, 2hrs	-0.57235	7.161	11.935	1594	0.046659	0.06191	0.39008
220°C, 2hrs	-0.5778	8.477	16.954	1319.1	0.051666	0.051324	0.55413
250°C, 2hrs	-0.50949	9.1822	15.304	1953.7	0.076984	0.089128	0.50019

From the above data, it was found that corrosion rate is lower **0.11868 mm/year** in case of Base sample and demonstrated a high level of corrosion resistance with its broad passive region and low corrosion current density. In the H_2SO_4 acidic solution, al-alloy 6063 at $220^{\circ}C$, 2 hours also showed a very high corrosion current density and a short passive zone, indicating limited corrosion resistance. According to the Tafel analysis, the sample corrodes with a relatively high rate and susceptible to localized corrosion attack.

The authors Aluru Praveen Sekhar and Debdulal Das [21] in a research article published in April 2019 regarding comparative assessment of Corrosion behaviour of Under-aged, Peak-aged and Over-aged Al-6063 alloy wherein it was concluded that Pitting corrosion and depth of intergranular corrosion (IGC) increased linearly during immersion tests in 0.1M ortho-phosphoric acid (H_3PO_4) solution. The dominant mode of corrosion in under-aged alloy was identified as localized pitting corrosion, while peak-aged is highly susceptible to IGC and in case of over-aged alloy extensive pitting corrosion was observed due to presence of solute cluster β'' (Mg_5Si_6), formation of β' Mg_2Si precipitates & galvanic reaction between AlFeMnSi particles.

A group of researcher Dmitry S. Kharitonova, Illia Dobrydena Birhan Seferd, Jacek Rylf, Angelika Wrzesińska, Irina V. Makarovah, Izabela Bobowska, Irina I. Kuriloi, Per M. Claessona [18] has opined that “Pure Al has a relatively strong corrosion resistance because of the adherent and dense oxide coating that forms spontaneously. On the other hand, the surface layer of Al alloys has a lot of heterogeneities, like intermetallic particles (IMPs). Because these IMPs produce local cathodes or anodes in the microstructure of the material, they make the material more prone to localized corrosion. Because of this, protecting Al alloys from corrosion is crucial and necessitates the creation of several protection techniques.”

In the present study, obtained hardness values as stated in chapter 5, sub-para 5.3 (figure: 19), sample with age-hardening temperature $120^{\circ}C$, 2hrs was identified as Under-aged, $170^{\circ}C$ to $220^{\circ}C$, 2 hrs as Peak-aged and $250^{\circ}C$, 2hrs as Over-aged condition. As shown in Table 11 & 12 corrosion rate in case of Peak-Aged sample observed very high **0.33368 to 1.3624 mm/year**, Under-aged sample in acid solution **0.21388 mm/year** and in 3.5wt% NaCl solution more corrosion resistant **0.0082629 mm/year**, similarly Over-aged sample more resistant in 3.5wt% NaCl solution **0.021402 mm/year**, however in acid medium it was observed higher value **0.50019 mm/year**. In both the medium corrosion rate of **base sample** was found **0.010065 and 0.11868 mm/year** which indicates more corrosion resistant than age harden samples. In sub-para 5.8, figure 38 and 39 microstructure in optical microscope after corrosion test has been shown, it was observed that extensive Pitting corrosion and localized corrosion occurred in case of Age-harden samples comparison to base sample.

Therefore age hardening treatment of AA6063 alloy is not preferable while using its in corrosive environment for prolong time of application in salt and acid medium because of effect on the Al surface through rapid dissolution of oxide film and material susceptible to pitting corrosion attack. The corrosion behaviour is also significantly influenced by the type of corrosive medium. In current work based on Tafel polarization test corrosion rate data, indicates AA6063 samples corrode more quickly in acid medium (H_2SO_4) than salt medium (NaCl). Although, corrosion in Al-alloy can be influenced by a number of variables like microstructure, distribution of second phases within the alloy and the electrochemistry of the alloy.

CHAPTER - 6

- **CONCLUSION**
- **FUTURE SCOPE OF WORK**

6.0 Conclusion:

In this work, microstructure and corrosion behaviour of age hardened Al 6063 Alloy was studied in details. Al 6063, T6 sample supplied by the private firm was undergone artificial age hardening with different temperature 120°C, 170°C, 220°C & 250°C and holding time in each sample was fixed 2 hours. After characterization of the samples by various test and technique such as optical microscopy, micro-hardness, FESEM, XRD and open circuit corrosion potential test following conclusions are drawn:

The microstructures of AA6063, T6 and age harden samples changes with increase in temperature during age hardening process. Alpha-Al and less amount of intermetallic compounds were traceable on the surface of Al matrix.

The micro hardness value observed highest 100 HV after aging temperature 170°C and was identified as peak aged condition, under-aged and over-aged condition also identified, therefore an ideal route to improve mechanical properties of AA6063 alloy is to perform ageing treatment for the precipitation solute atom within the alloy matrix, however optimization of two parameters temperature and time is important to obtain reasonable strength. Age-hardening Al-alloy 6063 can be utilised in automotive, aerospace industry, structural, architectural work where high strength is one of the criteria.

In present work, it is observed that the corrosion behaviour is significantly influenced by the type of corrosive medium. Based on the result obtained by Tafel polarization test, AA6063 samples corrode more quickly in acid medium (H_2SO_4) than salt medium (NaCl). The corrosion loss in 3.5wt% NaCl solution and 0.1M H_2SO_4 Solution of age hardened samples increases than base sample due to solute clusters. Age-hardened AA6063 alloy is not preferable while using in corrosive environment in salt and acid medium due to susceptibility to pitting corrosion or localized corrosion attack. Although, corrosion in Al-alloy can be influenced by a number of variables like microstructure, distribution of second phases within the alloy and the electrochemistry of the alloy.

Future Scope of Work:

In this study one set of age hardening temperatures were selected (120°C to 250°C), aging period was kept fixed 2 hours. Several earlier researchers have focused on issues regarding combination of different temperature and aging period to control its properties and microstructure and corrosion behaviour. Therefore further experiment can be carried out with different set of temperature and time. Another aspect pertaining to mention here that, proper solution treatment is required before age hardening process of Al-alloy.

References:

- [1] Prof Rajesh Prasad, IIT Delhi NPTEL Y-Tube lecture on Introduction to Material Science and Engineering in 2017
- [2] (Ref. www.elsevier.com# 2000 Elsevier Science S.A. All rights reserved)Journal of Materials Processing Technology 102 (2000) 234±240Ra®q A. Siddiqui*, , Hussein A. Abdullah, Khamis R. Al-Belushi Department of Mechanical and Industrial Engineering, Sultan Qaboos University, PO Box 33, Muscat-123, Oman Accepted 17 December 1999.
- [3] (Higgins, 2001; Khalifa, 2009)
- [4] (Hatch, 1984; ASM, 2005)
(Scamans, 1987; Kiourtsidis&Skolianos, 2007)
(David, 1987; Alaneme, 2010)
(Alaneme, 2011; Hutchings et al., 2000)
(Zhu &Hihara, 2010)
(Nnuka, 2000; Singla et al., 2009; AST, 1994; Pinto et al., 2009)
(Nunes&Ramanathan, 1995)
- [5] Corrosion of Aluminium and Aluminium Alloys, J.R. Davis, Ed., ASM International, 1999
 - ASM Specialty Handbook: Aluminium and Aluminium Alloys, J.R. Davis, Ed., ASM International, 1993
 - Aluminium and Aluminium Alloys, in Metals Handbook Desk Edition, 2nd ed., J.R. Davis, Ed., ASM International, 1998, p 417–505
 - D.G. Altenpohl, Aluminium: Technology, Applications, and Environment, 6th ed., The Aluminium Association Inc. and TMS, 1998
 - Aluminium: Properties and Physical Metallurgy, J.E. Hatch, Ed., American Society for Metals, 1984.
 - Maryam Mehdizade, Ali Reza Eivani*, Mansour Soltanieh
School of Metallurgy and Materials Engineering, Iran University of Science and Technology, Tehran, Iran
- [6] Google scholar [www.sciencedirect.com] & [researchgate.net]
- [7] Material Science & Engineering, 2nd edition, Willam D.callister,Jr. David G. Rethwisch adapted by R. Balasubramaniam, 2019, p 580- 604.
- [8] Authors. Aluru Praveen Sekhar*, Debdulal Das, Department of Metallurgy and Materials Engineering, Indian Institute of Engineering Science and Technology, Shibpur, Howrah - 711103, West Bengal, India
“Two-Body Abrasive Wear Behavior and Its Correlation with Mechanical Properties of Aged AA6063 Alloy” ResearchGate
All content of this page was uploaded by Debdulal Das on 21 January 2022.
- [9] F. A. Ovat¹, F. O. David¹ & A. J. Anyandi¹
“Corrosion Behaviour of Al (6063) Alloy (As-Cast and Age Hardened) in H₂SO₄ Solution”
Cross River University of Technology, Cross River State. P.M.B 1123, Calabar, Nigeria
Correspondence: F. A. Ovat, Cross River University of Technology, Cross River State. P.M.B 1123, Calabar, Nigeria. Tel: 234-803-859-9332. E-mail: fraijoe@yahoo.com

- [10] (Ref. www.sciencedirect.com)2003 Elsevier Science B.V. All rights reserved
M. Gavgali, Y. Totik*, R. Sadeler
“Effects of artificial ageing on wear properties of AA 6063 alloy”
Department of Mechanical Engineering, Faculty of Engineering, Ataturk University,
25240, Erzurum, Turkey Received 19 August 2002; received in revised form 6 January
2003; accepted 15 January 2003.
- [11] (Ref. www.elsevier.com)Crown Copyright © 2009 Published by Elsevier B.V. All rights
reserved.
Authors AhmetMeyvecia , Ismail Karacana , Ugur C, aligülü b , HülyaDurmus, c,*
“Pin-on-disc characterization of 2xxx and 6xxx aluminium alloys aged by precipitation
age hardening”
a.Karabuk University, Faculty of Technical Education, Department of Machine
Education, Karabuk, Turkey
b.Firat University, Faculty of Technical Education, Department of Metal, 23119 Elazig,
Turkey
c.Celal Bayar University, Turgutlu Technical Vocational School of Higher Education,
Turgutlu-Manisa, Turkey
- [12] (Ref. www.elsevier.com# 2000 Elsevier Science S.A. All rights reserved)
Journal of Materials Processing Technology 102 (2000) 234±240Ra®q A. Siddiqui* ,
Hussein A. Abdullah, Khamis R. Al-Belushi
“Influence of Aging parameters on the mechanical properties of 6063 Al-Alloy”
Department of Mechanical and Industrial Engineering, Sultan Qaboos University, PO
Box 33, Muscat-123, Oman Accepted 17 December 1999.
- [13] Anawe PAL et al., Fayomi OSI ^{2,3*}, Popoola API²
“Adsorption Integrity of Pharma-ketoconazole on the Corrosion Behaviour of type
AA6063 Aluminium Alloy on High Pressure Gas Cylinders for Oil and Gas
Application”
Department of Petroleum Engineering, Covenant University, Ota, Nigeria
Department of Chemical, Metallurgical and Materials Engineering, Tshwane University
of Technology, Pretoria, South Africa
Department of Mechanical Engineering, Covenant University, Ota, Nigeria
- [14] Herman Pratiknoa
“Aging Treatment to Increase the Erosion-Corrosion Resistance of AA6063 Alloys for
Marine Application”
Department of Ocean Engineering, Faculty of Marine Technology, Institute Teknologi
Sepuluh Nopember (ITS), Campus ITS Sukolilo, Surabaya, 60111, Indonesia
- [15] Mohammad Salim Kaiser
“Corrosion behaviour of al-12si-1mg automotive alloy in acidic, alkaline and salt
media containing zr traces
Directorate of Advisory, Extension and Research Services
Bangladesh University of Engineering and Technology, Dhaka-1000, Bangladesh
E-mail: mskaiser@iat.buet.ac.bd

- [16] Marzieh Kishan Roodbari
“Effect of Microstructure on the Performance of Corrosion Resistant Alloys”
Light Metals, Silicon and Ferroalloy Production
Submission date: June 2015
Supervisor: Jan H alvor Nordlien, IMTE
Norwegian University of Science and Technology
Department of Materials Science and Engineering
- [17] Deepa Prabhu, Padmalatha*,
“Studies of Corrosion of Aluminium and 6063 Aluminium Alloy in Phosphoric Acid Medium”
Department of Chemistry, Manipal Institute of Technology, Manipal University, Karnataka 576104, India
- [18] Dmitry S. Kharitonova, Illia Dobrydena Birhan Seferd, Jacek Rylf,
“Surface and corrosion properties of AA6063-T5 aluminum alloy in molybdate-containing sodium chloride solutions”
Angelika Wrzesińska, Irina V. Makarovah, Izabela Bobowska, Irina I. Kuriloi, Per M. Claessona,
Division of Surface and Corrosion Science, Department of Chemistry, School of Engineering Sciences in Chemistry, Biotechnology and Health, KTH Royal Institute of Technology, SE-100 44 Stockholm, Sweden
Received 25 December 2019; Received in revised form 4 March 2020; Accepted 6 April 2020
Department of Chemistry, Electrochemical Production Technology and Materials for Electronic Equipment, Chemical Technology and Engineering Faculty, Belarusian State Technological University, 220006 Minsk, Belarus c Jerzy Haber Institute of Catalysis and Surface Chemistry, Polish Academy of Sciences, 30-239 Krakow, Poland
- [19] M.Baki Karamış, Halıcı
“The effects of homogenization and recrystallization heat treatments on low-grade cold deformation properties of AA 6063 aluminum alloy”
Erciyes University, Engineering Faculty, Department of Mech. Eng. 38039 Kayseri, Turkey b Selçuk University, Seydişehir Vocational College, Seydişehir, Konya, Turkey
Received 25 August 2005; accepted 9 June 2006
Available online 3 July 2006
- [20] Book, Principles and Prevention of Corrosion by Denny A Jones
- [21] Authors. Aluru Praveen Sekhar*, Debdulal Das,
Department of Metallurgy and Materials Engineering, Indian Institute of Engineering Science and Technology, Shibpur, Howrah - 711103, West Bengal, India
“Corrosion behaviour of under-, peak-, and over-aged 6063 alloy: A comparative study”
DOI 10.1002/maco.201910961
All content of this page was uploaded by Debdulal Das on 25th April 2019.